

WINDING EXPERIMENTS
ON NONUNIFORM THICKNESS WEBS

By

JARED WILLIAM GALE

Bachelor of Science in Mechanical Engineering

Brigham Young University-Idaho

Rexburg, Idaho

2009

Submitted to the Faculty of the
Graduate College of the
Oklahoma State University
in partial fulfillment of
the requirements for
the Degree of
MASTER OF SCIENCE
July, 2012

WINDING EXPERIMENTS
ON NONUNIFORM THICKNESS WEBS

Thesis Approved:

Dr. J. Keith Good

Thesis Adviser

Dr. Don A. Lucca

Dr. Rick J. Gaeta

Dr. Sheryl A. Tucker

Dean of the Graduate College

TABLE OF CONTENTS

Chapter	Page
I. INTRODUCTION.....	1
II. LITERATURE SURVEY	2
Winding Models.....	2
Research Objective	6
III. WINDING EQUIPMENT, INSTRUMENTS, AND RESULTS	7
3.1 Equipment and Instrumentation.....	7
3.1.1 High Speed Web Line (HSWL).....	7
3.1.2 Instrumented Core.....	8
3.1.3 Strain to Pressure Converting	10
3.1.4 Linear Displacement Transducer (LDT).....	12
3.1.5 Rho-Meter	14
3.2 Winding Test Methods.....	15
3.3 Winding Test Results.....	16
3.3.1 Pressure Tests.....	17
3.3.2 Outer Lap Radius Tests.....	18
3.3.3 Hardness Tests	20
IV. MEASURING WEB CHARACTERISTICS	24
4.1 Instrumentation	24
4.2 Thickness Measuring Method.....	28
4.3 Thickness Measuring Results	32
4.4 Material Properties.....	36
4.4.1 Young's Moduli E_{wt} and E_{wz}	37
4.4.2 Radial Modulus E_r	38
4.4.3 Other Material Properties.....	39

Chapter	Page
V. COMPARISON OF TEST AND MODEL RESULTS	40
5.1 Core Pressure Comparison.....	40
5.2 Outer Lap Radius Comparison.....	42
5.3 MeSys and Beta Gauge Maxiwinder Comparison.....	44
VI. DISCUSSION OF RESULTS, CONCLUSION AND FUTURE WORK	45
6.1 Discussion of Results.....	47
6.1.1 Winding Tests	47
6.1.2 Thickness Tests	47
6.1.3 Maxiwinder and Winding Tests Results	48
6.2 Conclusion	49
6.3 Future Work	50
6.3.1 Winding Tests	50
6.3.2 Thickness Tests	50
REFERENCES	52
APPENDIX.....	54

LIST OF TABLES

Table	Page
Table 1 Sector 1 strain values	11
Table 2 Strain to pressure equations	11
Table 3 Wrap lengths, average thickness, and number of points.....	29
Table 4 MeSys HSWL relationship	30
Table 5 Maxiwinder inputs	39
Table 6 Pressure errors.....	45
Table 7 Outer lap radius errors	45

LIST OF FIGURES

Figure	Page
Figure 1 Path through HSML	8
Figure 2 Inside instrumented core.....	8
Figure 3 Fully assembled core	9
Figure 4 Variable resistors	9
Figure 5 Strain indicator and switches.....	10
Figure 6 Calibration chamber	11
Figure 7 Sector 1 calibration chart.....	11
Figure 8 LDT on track	12
Figure 9 Repeatability of LDT.....	13
Figure 10 Averaged bare core.....	13
Figure 11 Accuracy of LDT.....	13
Figure 12 Taking hardness tests.....	15
Figure 13 Rho meter on calibration block	15
Figure 14 Results core pressure	18
Figure 15 Results outer lap radius	20
Figure 16 Results hardness	21
Figure 17 Stacked average winding test results.....	23
Figure 18 MeSys mounted on driven track.....	25
Figure 19 MeSys Repeatability.....	25
Figure 20 MeSys Error.....	26
Figure 21 LED emitter and receiver	27
Figure 22 Tabs around roll.....	27
Figure 23 CMD scans sampling distances Tab 3.....	31
Figure 24 CMD scans sampling distances Tab 8.....	31
Figure 25 Averaged CMD thickness variation	33
Figure 26 Composite CMD compared with CMD scans	34
Figure 27 Composite CMD compared with CMD scans new sectors	35
Figure 28 Averaged MeSys thickness compared with averaged Beta gauge	35
Figure 29 Contour plot of MeSys thickness data.....	36
Figure 30 Stretch tests setup	37
Figure 31 Stretch test plot.....	38
Figure 32 Instron compression test.....	38
Figure 33 Stack compression with Pfeiffer curve.....	39
Figure 34 Core pressure tests and Maxiwinder.....	42
Figure 35 Outer lap radius tests and Maxiwinder.....	43

Figure	Page
Figure 36 MeSys vs Beta gauge compare pressure	44
Figure 37 MeSys vs Beta gauge compare outer lap radius	45
Figure 38 Core pressure throughout the roll radius sector 13.....	46
Figure 39 Core pressure throughout the roll radius sector 18.....	46

CHAPTER I

INTRODUCTION

A web is a material that is extremely long when compared with its width, and even more so when compared to its thickness. Web handling is the transport of webs through machinery where web processes occur that add value to the web. Web materials include plastic films, paper, textiles which may be woven or nonwoven, and metal foils. Web processes include coating, printing, laminating and surface treatments such as calendaring and corona treating. Each web may undergo several web processes before it is converted to a final product. Webs are commonly stored between processing in the form of a wound roll. Storage is required because processes occur at different velocities and because these processes may occur at different manufacturing sites around the world. Winding can be responsible for damage and, in some cases, loss of the web. Webs may have non-uniformity in thickness. This variation in thickness maybe in the length dimension (called the Machine Direction) or in the width dimension (called the Cross Machine Direction). These directions are abbreviated as MD and CMD. This thickness variation may have occurred when the web was formed or later when it was coated. These thickness variations can cause stress variations when winding. This is the topic of this thesis

CHAPTER II

LITERATURE SURVEY

Winding Models

The first winding models ignored web thickness non-uniformity; these models were one-dimensional in the radial direction in the wound roll. These models would provide outputs, including the pressure and circumferential stress as a function of radius. Inputs included web material properties, core properties, and winder operating tension. These early models were called center winding models because the torque was applied to the center of the roll, called the core. Cores can be composed of paper fibers and resin, but can also be composed of plastic or metal too. As these models developed, more complex material behaviors were allowed. A thorough review of these models are given by J.K. Good [1].

One of the most thorough elastic web winding models was developed by Z. Hakiel [2]. Hakiel treated the web as an elastic orthotropic material. The winding model assumed plane stress conditions and required inputs of Young's Modulus in the radial and circumferential directions. One Poisson ratio was required which was assumed small from measurements, and the other was determined from Maxwell's relation. Instead of the Archimedean spiral geometry, he assumed the

web could be added to the roll in the form of concentric hoops for simplicity. Hakiel understood the contact mechanics of web surfaces subject to pressure. To accommodate this he posed the geometric nonlinearity in the form of a radial modulus that was state dependent on contact pressure. His one-dimensional model was a second order differential equation in pressure with respect to radius with non-constant coefficients due to the radial modulus dependency on pressure. Since the coefficients varied, the differential equation was solved numerically for the increments in pressure due to the addition of the most recent hoop. Two boundary conditions were required for each numerical solution. The first boundary condition considered compatibility between the radial deformation of the outside of the core and the first lap of web material added to the core. Through constitutive relations this could be posed as a derivative boundary condition (pressure with respect to radius) at the core. The second boundary condition was derived from equilibrium of the outer lap. The web tension stress in the web just upstream of the winder is assumed to be known. It is then assumed that tensile stress is equal to the membrane circumferential stress in the outer lap. Equilibrium is then used to relate that circumferential stress to the pressure beneath the outer lap. With these boundary conditions, the second order differential equation could be solved for the increments in pressure due to the addition of the most recent lap in each web layer. These increments in pressure are added to the previous increments in pressure that resulted from the addition of earlier laps to the roll from the total pressure in each lap. The total pressure is then used to update the radial modulus in each lap prior to the next solution of the differential equation. This process continues until all the laps have been added to the roll. When this is complete, the radial stress (pressure) is known as a function of the radius, and hence the derivative of the radial stress with respect to pressure is known too. The equilibrium expression in polar coordinates can then be used to infer the circumferential stress as a function of radius. Hakiel verified his model on uniform thickness webs that had been wound into narrow rolls. He measured the axial force required to cause slippage in the roll and with a known friction coefficient was able to infer the pressure of contact. By using a set of dies he was

able to induce slippage at varied radius in the completed roll and infer the total pressure at those radii and compare them to the output of his model.

Hakiel's next contribution to the winding literature [3] addressed web non-uniformities. He extended his previous one-dimensional model to a two-dimensional model by assuming the one-dimensional model could be used to model several CMD segments across the entirety of the roll width. As a function of varied thickness non-uniformity, the outer wrap radius of each CMD segment could vary, and he developed means to allocate the total web tension to the CMD segments as a function of outer lap radius. All of the input needed for his original model was required, but now the thickness variation across the web width was required. Hakiel conducted center winding tests at two tension levels on two different webs. After testing was complete, he harvested 30 CMD strips of web for each of the two webs. A contacting thickness gauge was used to evaluate the web thickness variation across the web width for each strip. These thickness variations were then averaged in the MD to produce one chart of thickness variation over the web width for each of the two webs. It was assumed that this average thickness variation persisted down the entire length of web wound in the MD. Hakiel documented the results of his winding trials with two test methods. He developed an instrumented core. This core was composed of several segments (10) in the CMD and each segment was supported by guide pins so it would remain concentric on the winder shaft. These segments were instrumented with strain gauges, such that the final total pressure at the core could be measured at 10 equally spaced CMD locations. He also had a contacting profilometer, with which he could trace the radius profile of the outer lap with respect to CMD location. Thus, Hakiel had core pressure and outer lap profile data, which he could compare to the output of his wound roll model. For the test cases, he had good agreement between test and model core pressures. That agreement improved later when he developed an improved algorithm to allocate the web tension to the CMD sectors that were individually treated with his one-dimensional model [4]. His comparisons between test and model

for the outer lap profile were not as good. Trends were verified, but much of the detail measured was not witnessed in the model results.

Kedl [5] developed a model similar to that of Hakiel [3] to account for widthwise thickness non-uniformity. It too broke the web width into sectors and modeled each sector with a one-dimensional roll model and also developed a formula to allocate the web tension dependent on sector outer lap radius. In the laboratory, Kedl used a Beta gauge to infer web thickness. The Beta gauge is composed of a radiation source on one side of the web with a collector on the opposite side. The radiation is attenuated by the mass of the web between the emitter and the collector. The emitter/collector is mounted on a CMD traverse, which moves back and forth across the web at constant velocity while the web is transported at a constant velocity in the MD. The thickness data is thus acquired in a zig-zag trace of the web. Kedl did not publish his thickness data making comparisons at a later date impossible. Kedl used sensors called force sensitive resistors¹ to measure in-roll pressures at various wound roll radii and CMD locations. He compared the average of all pressures taken at a particular CMD location, but at various radii, to similar averages taken from his model output.

Mollamahmutoglu developed a two-dimensional axisymmetric wound roll model [6]. This model differs from those of Hakiel and Kedl in that compatibility of the deformation is ensured for a given layer across the web and roll width. He was first to extend two-dimensional models to incorporate the potential for an impinged nip roller at the outside of the winding roll [7]. This roller prevents the web tension from being allocated solely on the outer lap radius across the roll width. This roller can induce slippage in the outer laps of the winding roll, making the total tension in the outer lap exceed the web tension. To verify this model, an instrumented core and a device to measure the outer lap radius with respect to CMD location were developed², similar to

¹ InterLink Electronics, Santa Barbara, CA.

² Mr. Ron Markum, Research Engineer, Web Handling Research Center, Oklahoma State University.

that described by Hakiel. Some verification was accomplished using limited webs with limited thickness data. The axisymmetric winding model was first verified by comparison to test data from Hakiel [3].

Research Objective

To document first the characteristics of a non-uniform web including thickness and modulus. To use that web in center winding tests for cases with and without a nip roller applied. To use the model developed by Mollamahmutoglu with the measured web characteristics and compare the model output to the data acquired during the winding tests.

The research objectives are:

- Document the characteristics of a non-uniform web including thickness and modulus.
- Perform center winding tests, on the same web, with and without a nip roller load applied.
- Use the model developed by Mollamahmutoglu with the measured web characteristics and compare the model output to the data acquired during the winding tests.

CHAPTER III

WINDING EQUIPMENT, INSTRUMENTS AND RESULTS

3.1 Equipment and Instrumentation

Some of the data acquisition tools used to validate the finite element model were unique and will be discussed in their own section. A brief physical description and mechanics of the tool, manufacturer specifications (when applicable), and the repeatability of their measurements as installed in the Web Handling Research Center (WHRC) will be given.

3.1.1 High Speed Web Line (HSWL): This is the machine in the WHRC that ran the web and used the path seen in Figure 1. The speed control on this machine is extremely accurate because of the feedback loops that were programmed into the drives. Once the machine is up to speed, which takes less than a second, it only varies by +/- 1 ft/min. Another important input into the HSWL is the tension that is maintained on the web.

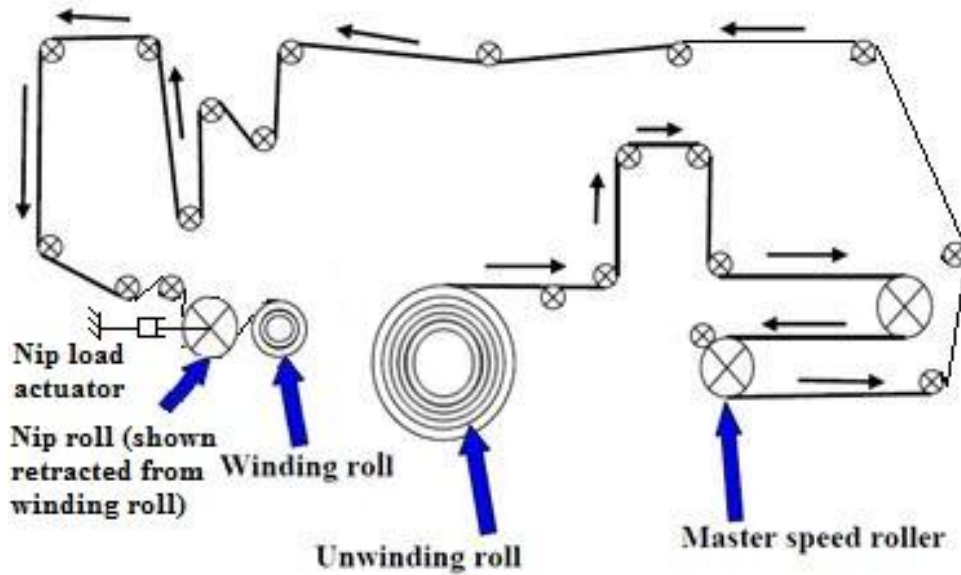


Figure 1 Path that the web travels through the HSWL

3.1.2 Instrumented Core: This instrument was created by precisely machining the outside of an eight-inch diameter piece of aluminum, slicing it into one inch high sections (sectors) and machining holes in it (Figure 2). After the machining, four strain gauges were attached to the inside of each piece and wired together in a Wheatstone bridge. These 24 wired sections were slid onto a core and wired onto a variable resistor, which was used for balancing the bridges. They were also wired to output posts so that a strain indicator could easily be attached and the strains read (Figures 3, 4).

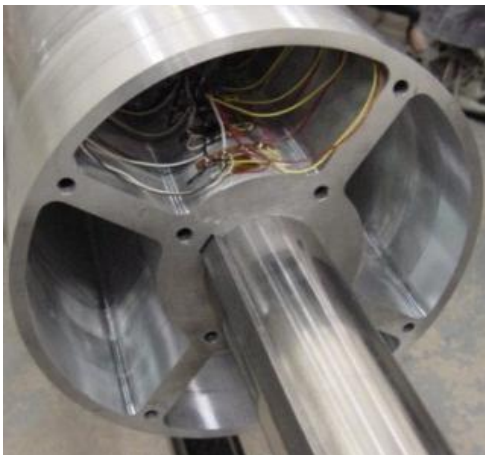


Figure 2 Inside the instrumented, segmented core

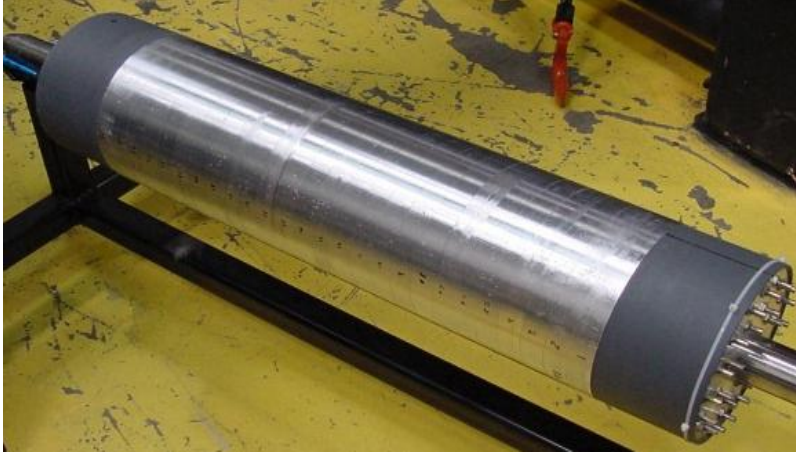


Figure 3 Fully assembled core



Figure 4 Variable resistors for balancing the sectors

Before wrapping any web on the core, lead wires from the strain indicator (3800 Wide range Strain Indicator Measurements Group Instruments division) were run from the core to their respective locations (Figure 5). Using an excitation voltage of 5 and a gauge factor of 2.13, the strain gauges in each of the sectors were balanced by adjusting the resistances. This balancing was done before each of the windings in which core pressure would be measured.

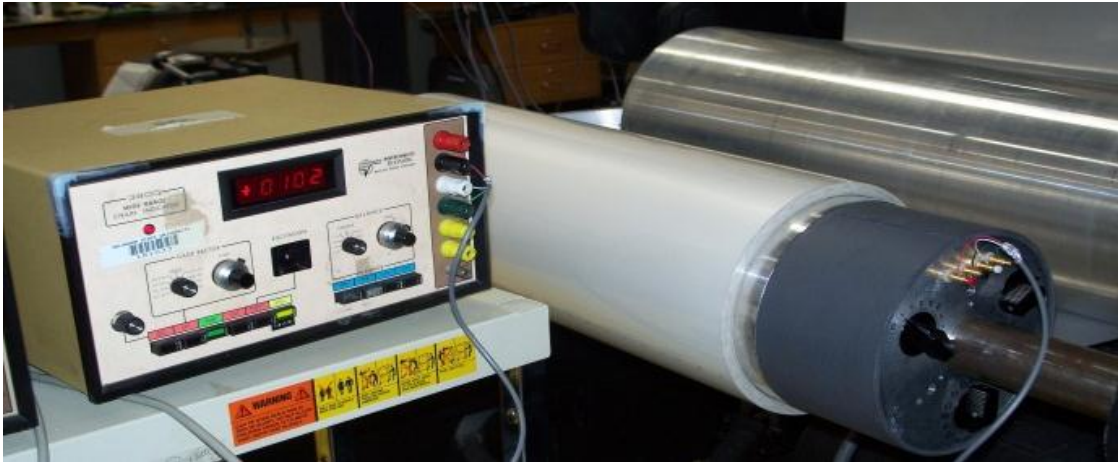


Figure 5 Strain indicator and switches to change from sector to sector

3.1.3 Strain to Pressure Converting: A custom tool was created to convert the read strains into pressure values. A steel tube with flanges on each end had a dummy core placed in it and was filled with liquid rubber. Once the rubber dried, a pressure regulator and gauge were attached to the tube (Figure 6). This was placed on the instrumented core, and the bladder was inflated using compressed air in ten-pound increments. The strains for each of the 24 sectors were recorded and plotted. Using the equation of the best-fit linear curve in Excel, a relationship between pressure and strain was found for each sector. See Table 1 for sector 1's strain values and Figure 7 for an example of the excel plot with the trend line and equation shown. Table 2 shows all the relationships, with "x" equaling strain.

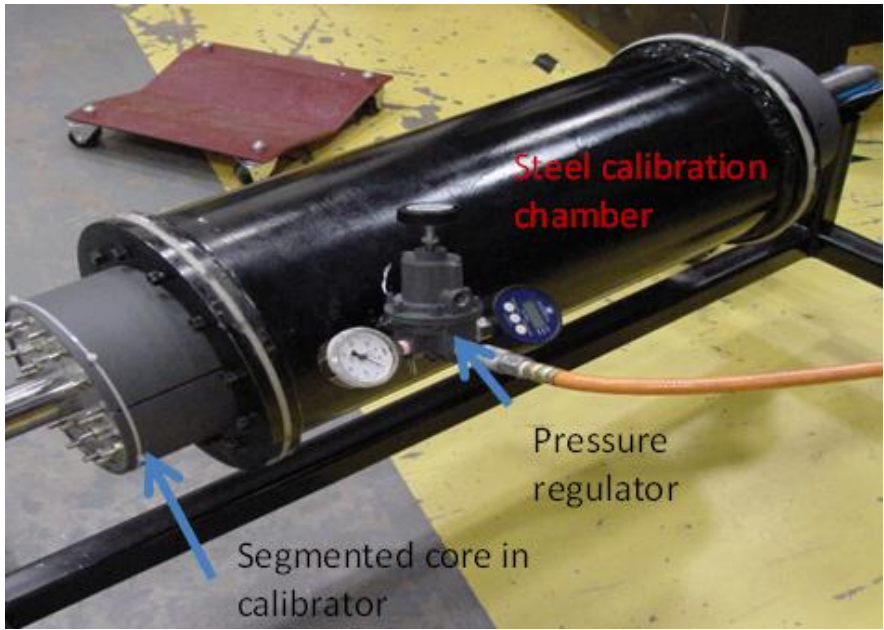


Figure 6 Calibration chamber

Table 1 Sector 1 strain values

Strain (in/in)	Pressure (psi)
60	10
112	20
163	30
213	40
265	50
316	60
367	70
418	80
470	90
521	100

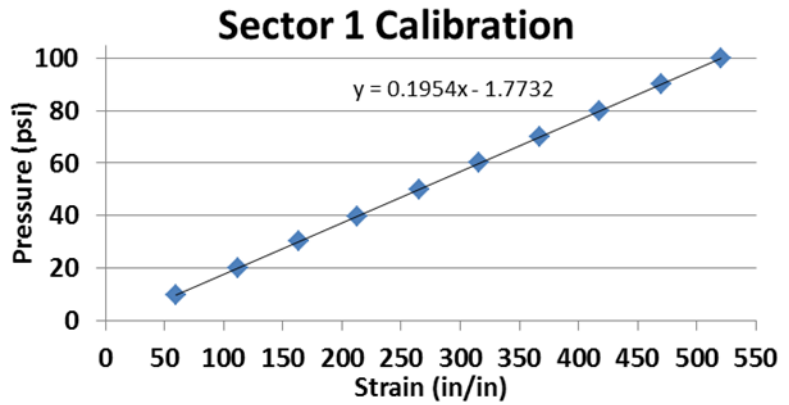


Figure 7 Plot of the values of Table 1

Table 2 Strain to pressure equations

Sector	Equation of line	Sector	Equation of line	Sector	Equation of line	Sector	Equation of line
1	0.1954x - 1.7732	7	0.1981x - 0.5457	13	0.1947x - 0.8536	19	0.1957x + 0.1658
2	0.1959x - 0.1345	8	0.197x - 0.0454	14	0.1872x - 0.5746	20	0.1934x + 0.1347
3	0.1954x - 1.9686	9	0.2128x - 0.6383	15	0.1896x + 0.4231	21	0.1996x - 0.4297
4	0.201x - 0.5379	10	0.1964x - 0.6028	16	0.1992x - 0.4589	22	0.2041x - 0.2041
5	0.194x - 1.2969	11	0.2023x - 0.014	17	0.1889x + 0.1758	23	0.1938x + 0.358
6	0.1991x + 0.0987	12	0.2156 - 0.3443	18	0.1998x - 0.7364	24	0.210x - 1.0826

3.1.4 Linear Displacement Transducer, LDT – LD 500-5 (radial profile tool): The concept of this tool is very simple: a foot is attached to a spring-loaded position sensor and, as the foot moves up and down, the location of the foot is read. In the WHRC, the tool is mounted on a track above the core, can be adjusted up and down, and is manually moved across the profile of the specimen (Figure 8). The tool used for these experiments was manufactured by Omega Engineering and boasts a repeatability of 4 micro inches (.000004 in) [8]. Because the tool was not used in ideal conditions, the repeatability of the experiment was checked. Four tests were run on the same location of the bare instrumented core; results displayed in Figure 9. The correlation between the tests was shown to be good. Also seen in the plot is a general upward trend in the data, meaning the tool track and the core were not completely parallel. To adjust the data for this offset, six scans were made around the bare core and averaged (Figure 10). This average was subtracted from all the outer lap radius data. The accuracy of the LDT was checked by taping known thicknesses (a piece of 300 gauge web and 100 gauge shim stock) on the roll and comparing these with the roll profile without the steps (Figure 11).



Figure 8 LDT on track

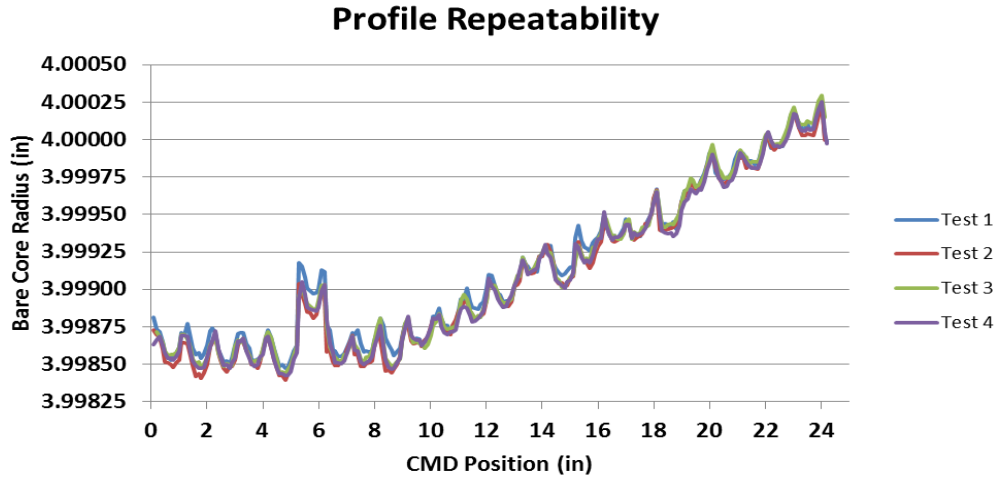


Figure 9 Repeatability of LDT

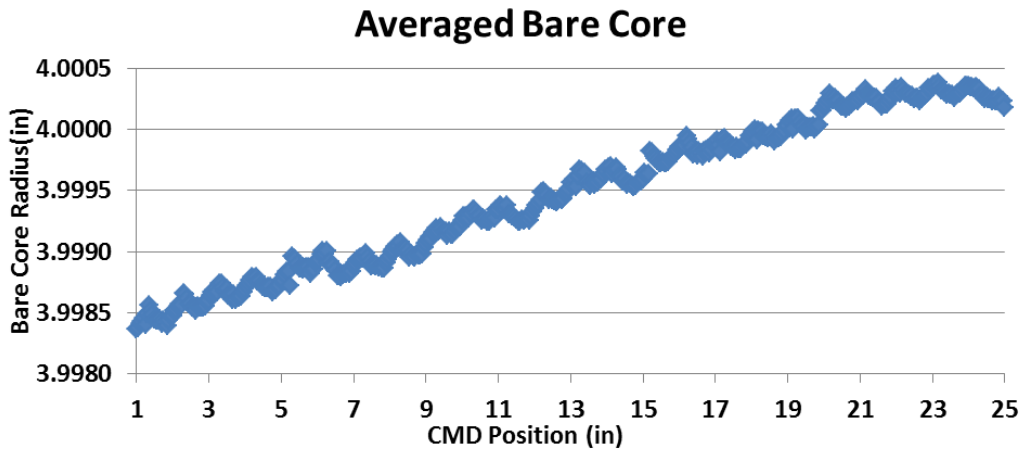


Figure 10 Averaged bare core

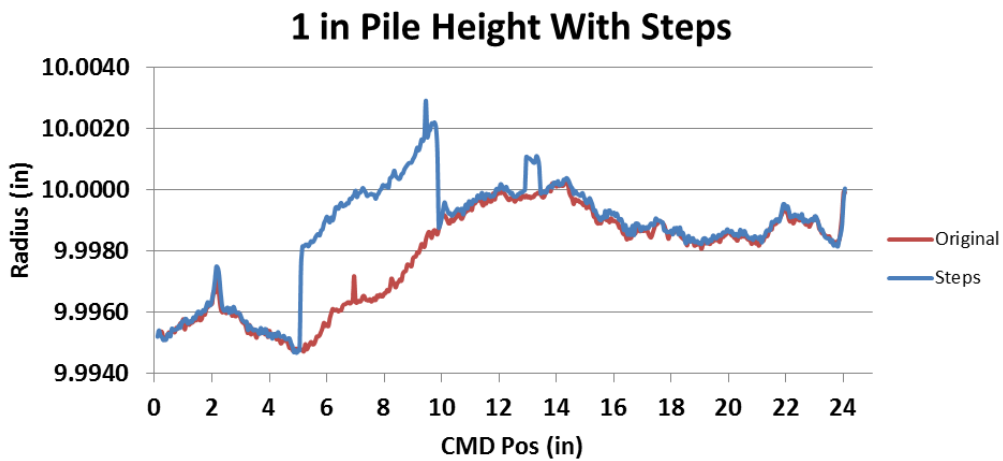


Figure 11 Accuracy of LDT

3.1.5 Rho-Meter: As layers are wrapped onto cores, different areas become harder than others due to the thickness variations adding together or creating voids. To measure this hardness, a Rho- Meter was used.

The Rho-Meter measures the peak force generated by contact of a striker moving at a known velocity against a surface of unknown hardness... This reactive force, or “impulse force”, rises from zero to a maximum value then returns to zero... This ‘impulse’ determines the ‘magnitude of the blow’ and is exactly equal to the net change in momentum of either body... Peak forces are measured by a high accuracy accelerometer... The peak force [is] ... displayed on the digital display. Greater hardness of the test object results in larger peak force and more peak acceleration [9].

The Rho meter is operated by holding its foot tangent to the roll and pulling the trigger (Figure 12). How the trigger is pulled affects the output. For example, if the trigger is pulled really quickly, then you would get a higher reading; while, if the trigger is pulled very slowly, a much lower value would be displayed. To account for this variability, a calibration block is included with the Rho meter and several tests were performed to learn the correct trigger pulling speed and force (Figure 13). The Beloit Rho-Meter that was used gives an accuracy rating of +/- 1 Rho. The Rho unit was created by the manufacture and is defined as a 3 g deceleration of the mas of the striker. However, due to the possibility of not always having the foot of the meter exactly tangent to the surface and the variability of trigger speeds, five samples were taken at each sector location and then averaged. The variation between most samples was better than +/- 10 Rho.



Figure 12 Taking hardness tests with Rho meter



Figure 13 Rho meter on calibration block

3.2 Winding Test Methods

The first step in validating the previous work was determining how much web needed to be wound on the core for each of the various tests. To begin, each of the sectors was balanced without any web on the core. Then the web was run through the HSWL at 15 ft/min with a web tension of 1pli (pound per linear inch). The machine was run at this low speed to minimize the effect of air being entrained between the layers, which would have given incorrect data. The machine was stopped when there was a half-inch of pile height on the core. At this point, the strains were recorded. The web was started again and run until another half-inch of pile height was gained. The strain was recorded after each additional half-inch of pile height. The test was

completed when the difference between the strains being recorded was minimal or, effectively, no longer changing. This occurred when there was a total of four inches of pile height. This test was only performed once, after the required pile height was known, the web was wound to four inches of pile height then tested.

After the length of web needed was determined, the web was wound with different winding configurations and tensions. First, the web was wound using center winding with multiple tests using web tension (T_w) at 1 and 1.5 pli tension settings. Next, a nip load (roller pressed against the roll as it wound) of 1 pli was applied and again multiple tests were run at 1 and 1.5 pli web tensions.

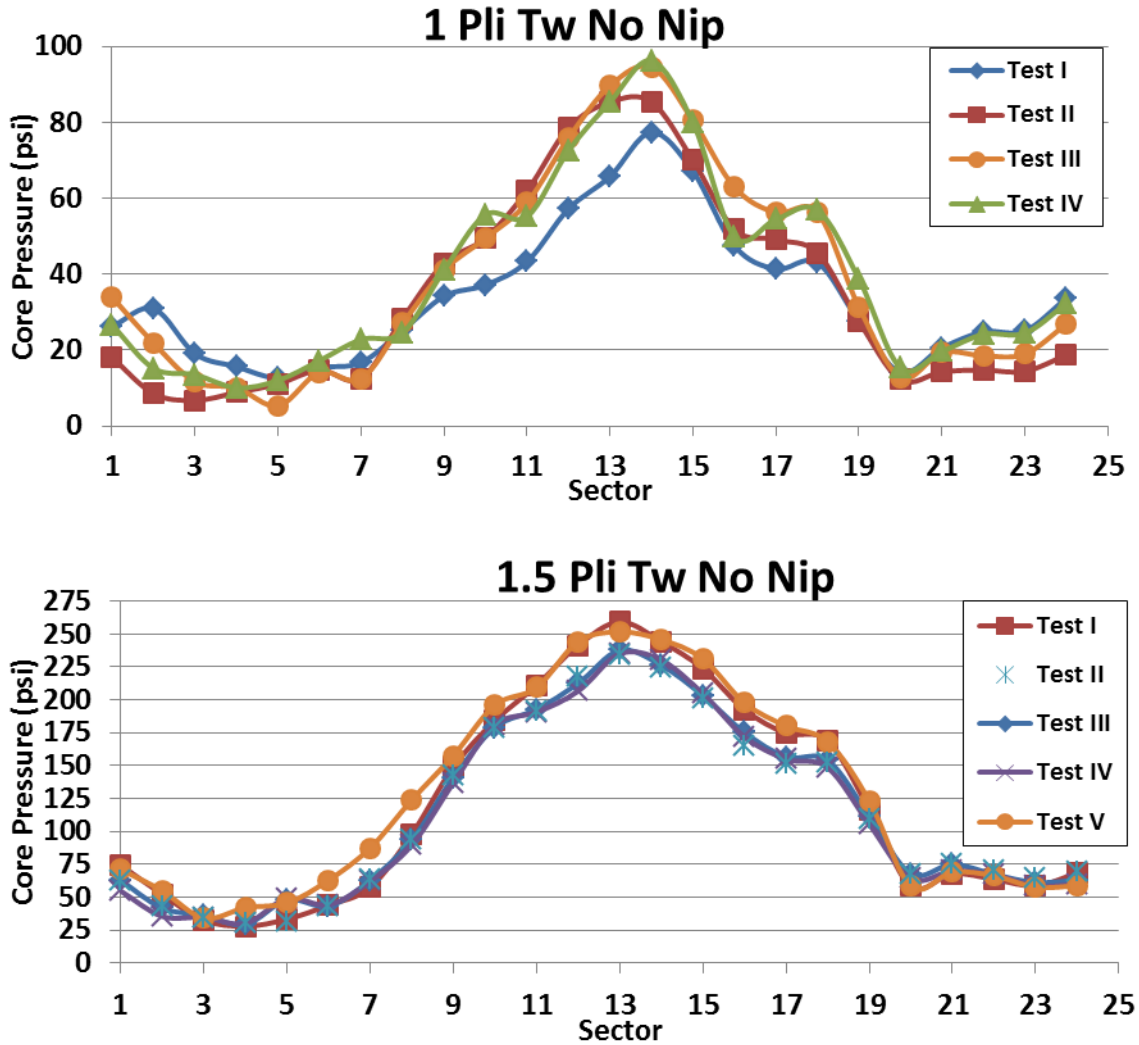
Once the rolls were wound, three different tests were conducted on the roll: the core pressure, outer lap radius, and Rho hardness. To collect the pressure values, the strain indicator was attached and the core was switched through the different sectors. The strain for each sector was recorded. Then, using the above mentioned strain to pressure conversion, the pressures were found. The next test done was obtaining the outer lap radius, which was conducted by moving the LDT across the roll. After the data was collected, the effect of the core was subtracted. The minimum value was then found and subtracted from the data without the core. By doing this, the profile of outermost layer could be seen and compared with other tests. The last test, evaluating the hardness of the roll, was conducted by using the Rho meter. Samples were taken from the middle of each of the sectors. Again, five samples were taken for each sector and then averaged.

3.3 Winding Tests Results

The results from each of the different tests for the four different configurations will be presented, followed by a comparison between the tests themselves. The tests will be presented in the following order: pressure, outer lap radius, and then hardness. All of these tests were performed after four inches of pile height was on the core.

3.3.1 Pressure Tests:

The pressures were found by reading the strains off the strain indicator and then converting them to pressures. The plots of the different tests are shown in Figure 14. It can be seen that there is great repeatability between the tests.



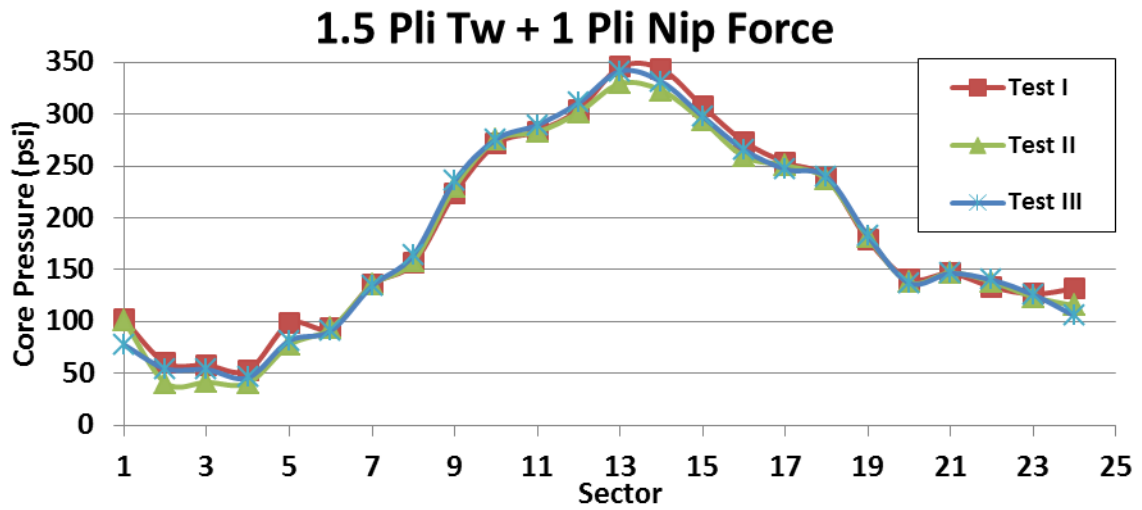
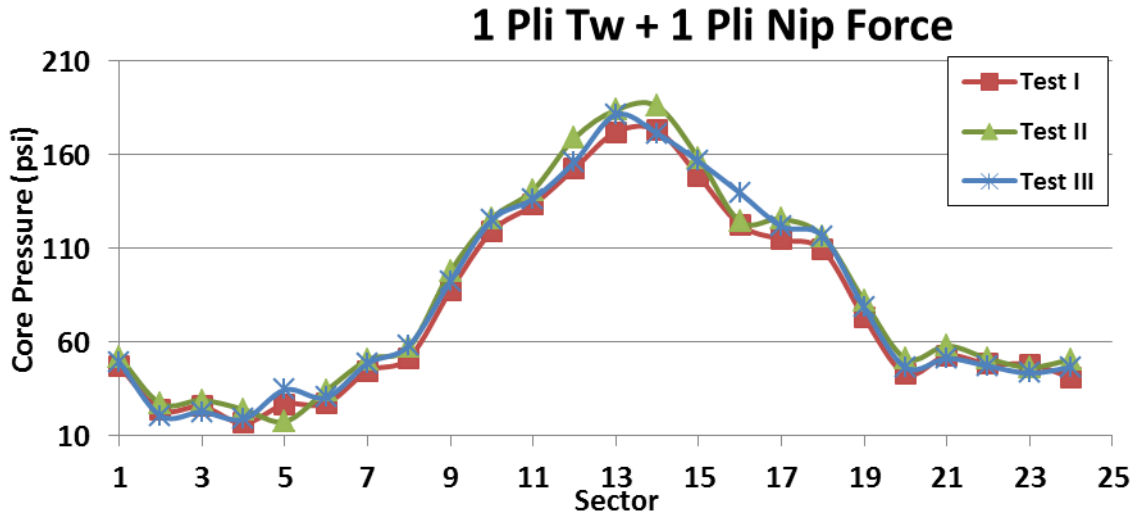
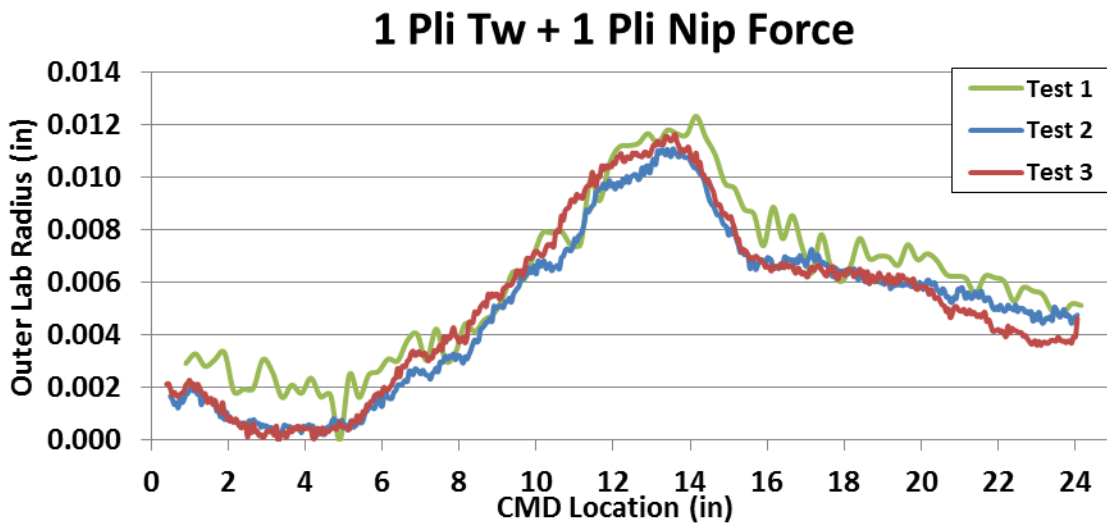
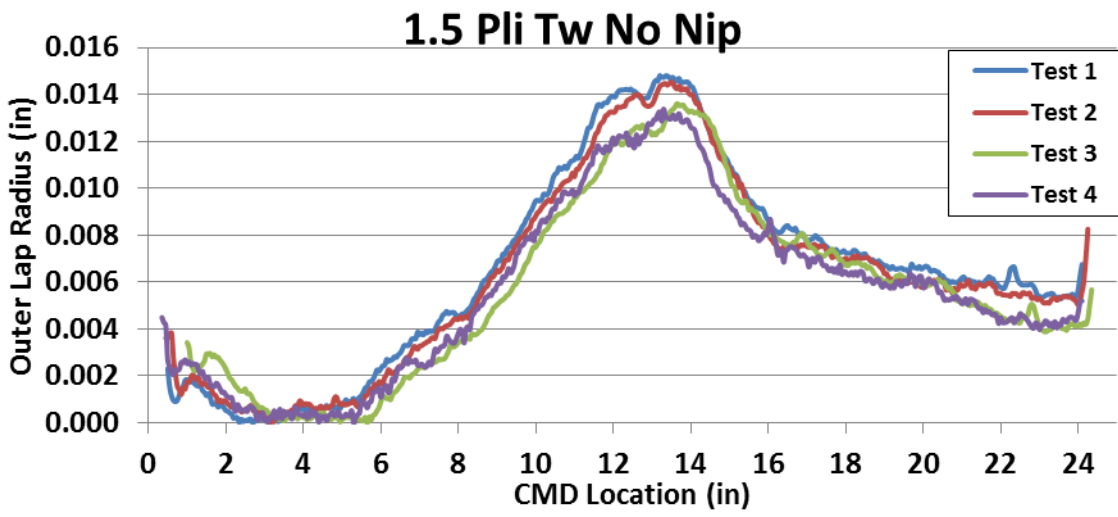
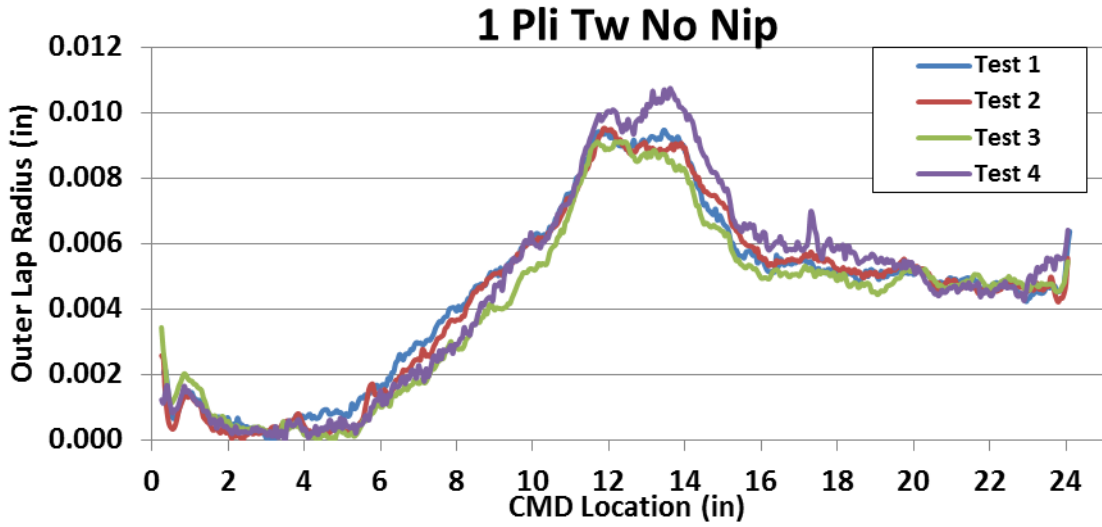


Figure 14 Results of core pressure tests

3.3.2 Outer Lap Radius Tests:

These were found by running the LDT across the outer profile of the roll. The plots of the different tests are shown in Figure 15. For test 1 of the 1 pli Tw + 1pli Nip Force case, the LDT lost ground, resulting in noise in the data. The values were averaged every 0.25 inch across the web in the CMD to eliminate a majority of the noise. Again, great repeatability is seen in these tests.



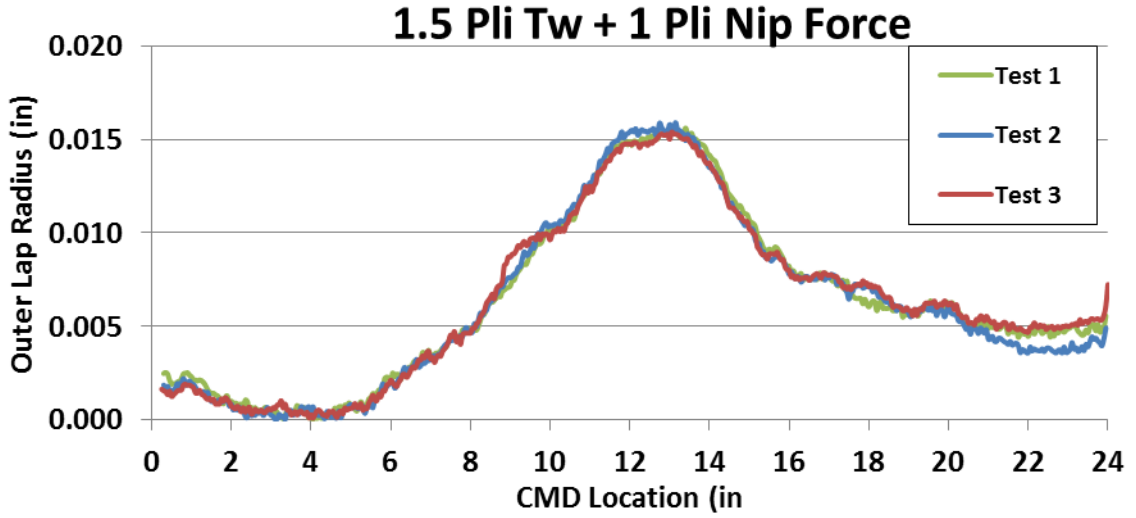
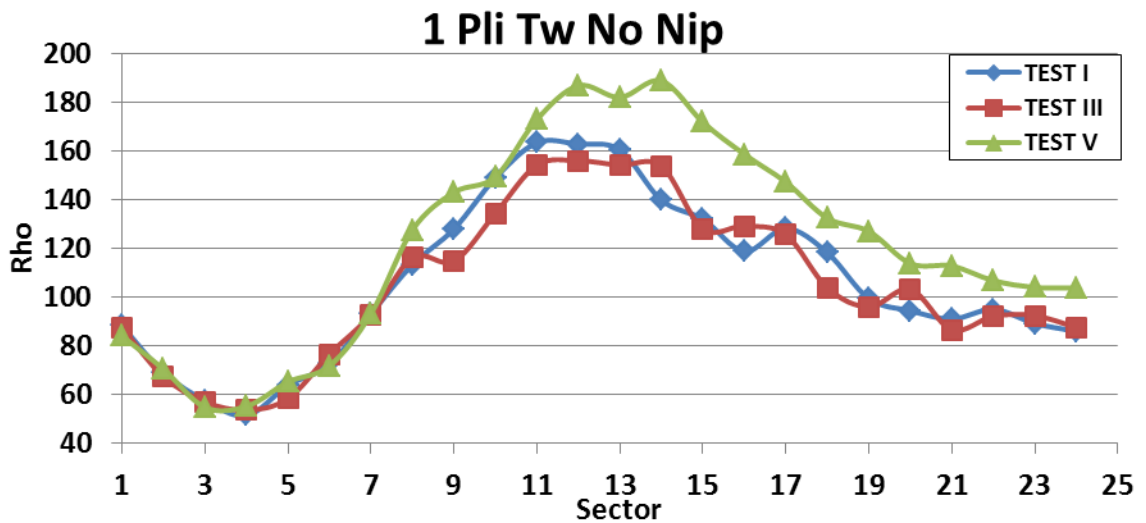


Figure 15 Outer lap radius versus CMD location

3.3.3 Hardness Tests:

The hardness was taken at the middle of each sector five times and then averaged. The plots of the different tests are shown in Figure 16. These tests had slightly less consistency than the pressure and outer lap radius tests.



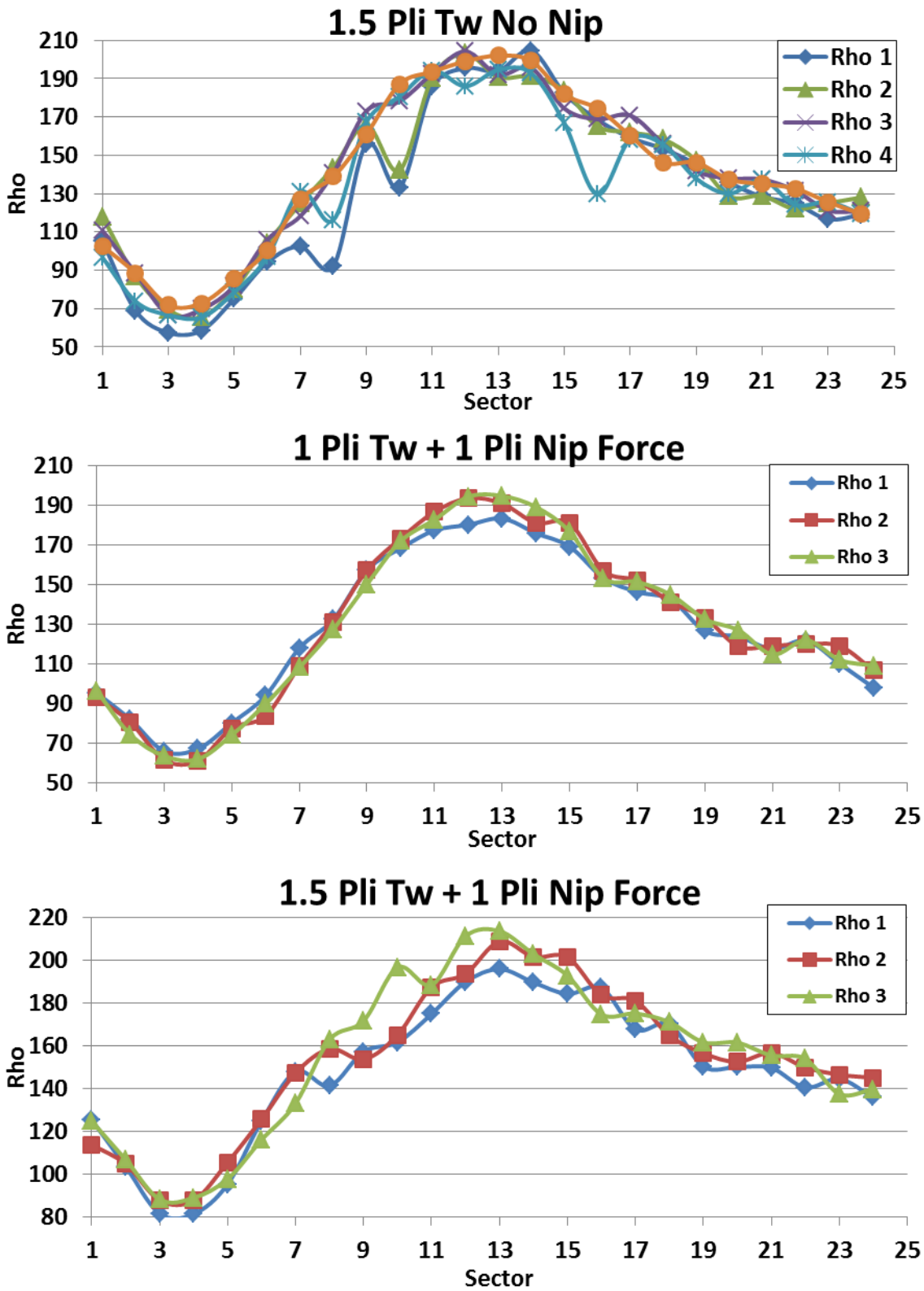
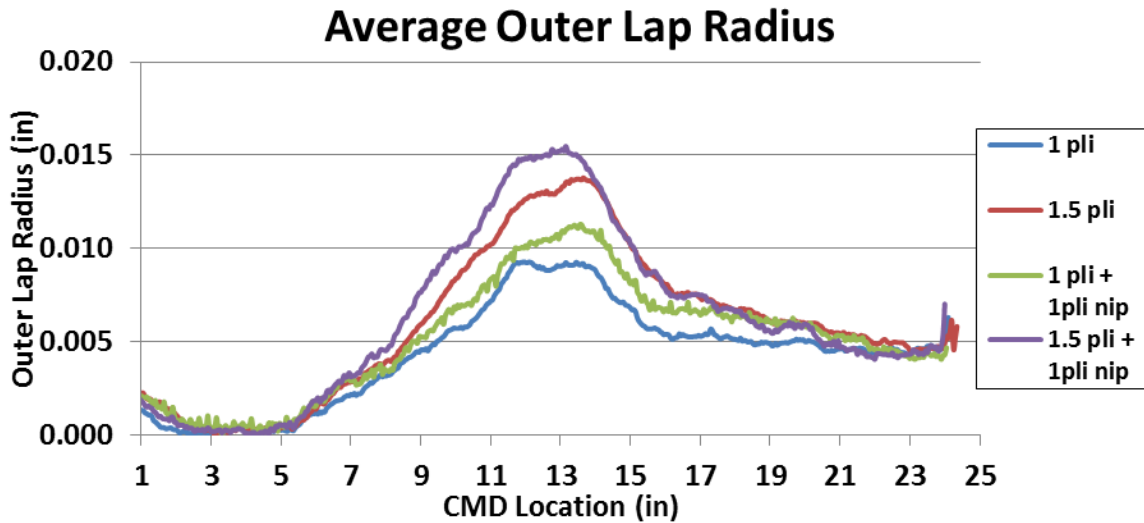
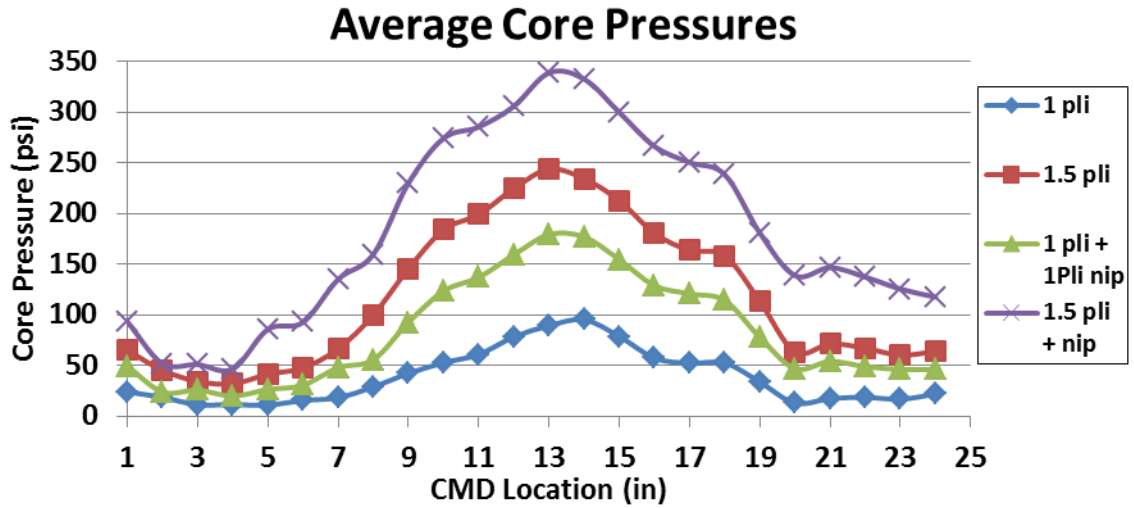


Figure 16 Results of hardness test

As seen in the plots above, the tests showed very good repeatability, which increased confidence in the test method and the equipment. The next plots (Figure 17) show the above data averaged and plotted together. It can be seen how each test had similar shape.



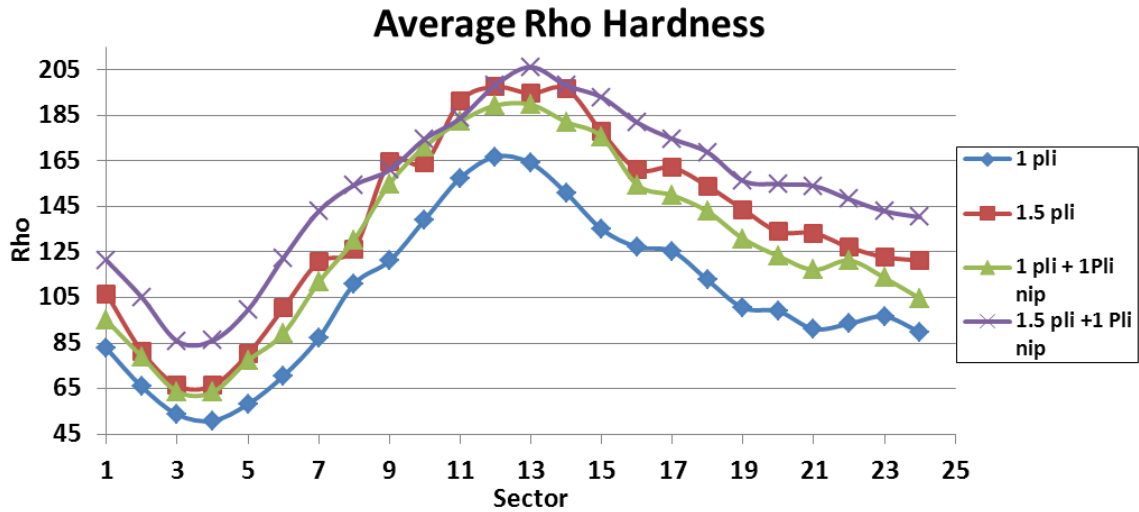


Figure 17 Stacked average winding test results

There is obviously some similarity between the pressure, the outer lap radius, and the rho hardness readings in Figure 17. In each case, the measurements peak in the vicinity of sector 13. Also note how each measurement shows a lower value for sectors 1 through 5 and for sectors 20 through 24 for each winding test case. The rho hardness readings vary with hardness of the outside of the roll. The striker on the rho meter strikes the outside of the roll and then deceleration of the striker is measured quickly before a stress wave could travel to the core and rebound to the roll surface. The deceleration is read in “Rho” units, an arbitrary unit selected by the inventor, and is defined as the 3 g deceleration of the mass of the striker. So it is interesting that the hardness at the exterior of the roll has a similar variation in the CMD as the core pressure at the inside of the roll, because they were four inches apart.

CHAPTER IV

MEASURING WEB CHARACTERISTICS

4.1 Instrumentation

The web thickness will be measured using a non-contact thickness gauge produced by MeSys GMBH³. The device works on the principles of attenuated ultrasound. A transducer, shown in Figure 18, transmits ultrasound toward the web. Some of the ultrasound is reflected and absorbed by the web's surface, but some ultrasound is transmitted through the web to a receiver on the other side of the web, opposite of the transmitter. The accuracy of the MeSys gauge is quoted as 0.5% of the thickness over a sampling diameter of 5 mm [10]. Before each test, the MeSys needed to be recalibrated. The procedure for doing this is as follows: The web was brought to the exact same location on the HSWL and set to 1 pli tension; then the data acquisition program would move the MeSys off the web, sample the air, and then move back to the middle of the web, where the MeSys would take a sample. In this way the receiver measures the ultrasound attenuated only by air and then compares that to the ultrasound attenuated by both air and the mass of the web. The user then provides the thickness associated with the web used as a calibration reference.

³ MeSys GMBH, Diessener Strasse 1, D-86919, Utting, Germany.



Figure 18 MeSys is mounted on a driven track

Similar to the radial profile tool, repeatability and accuracy tests were performed with the MeSys. First, the repeatability test was performed by running a short MD length of web (233 inches) at slow speeds on the HSWL and sampling as fast as possible with the MeSys. Two scans were performed and there was good correlation between them, so the method was considered correct (Figure 19).

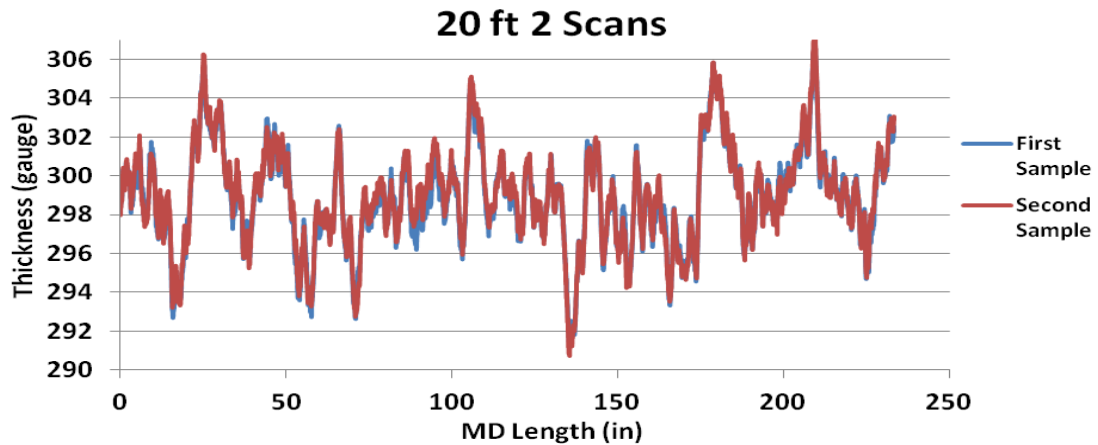


Figure 19 MeSys repeatability

To test the accuracy of the MeSys, a noise test (designed to measure outside interference on readings) was conducted by letting the MeSys test a single piece of web multiple times (Figure 20). The standard deviation in the points was found to be 0.14 gauge points, and the data had a

spread of about 0.8 gauge points. Again, MeSys quotes gauge accuracy as 0.5% of the nominal thickness. For a 300 gauge web, this would be 1.5 gauge units. From the data shown in Figures 19 and 20, the accuracy appears to be at least this good.

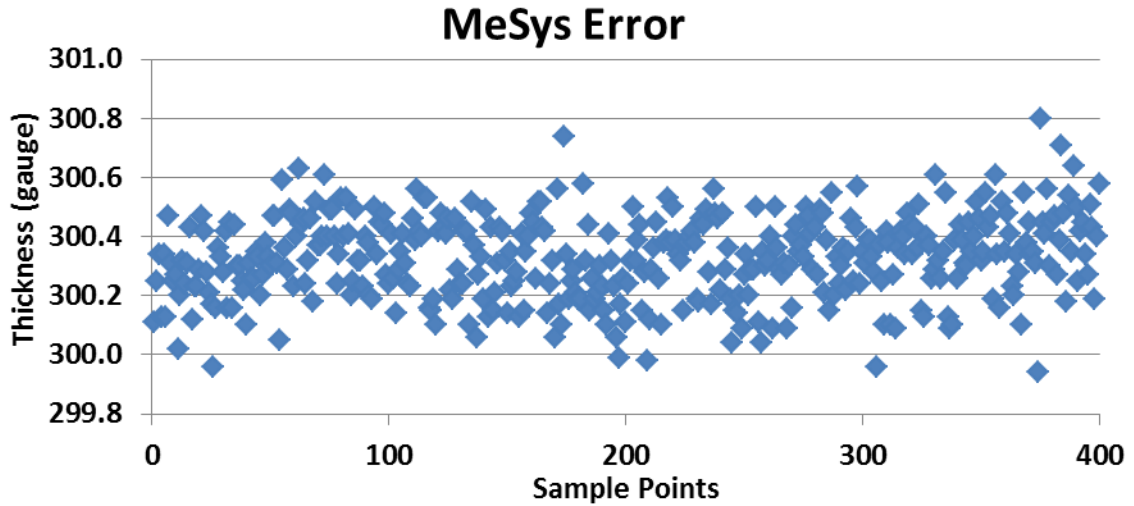


Figure 20 MeSys' error

Because of the potential for massive amounts of data being collected while running the MeSys, a system was developed for indexing the location of the web. The original idea was to use a clear web with dark spots marked at different locations on the web. When these marks would pass under the sensor, a voltage difference would be sent to the acquisition computer, thus marking the MD position (Figure 21). Then, as the MeSys was stepped across in the CMD, all these marks would be in the same position. After proving this concept, an opaque web was chosen for testing, which caused a constant closed condition from the photo sensors. To combat this change, the sensor was held off to the side of the web, and 3M flags (for marking pages) were used to trip the sensors. The flags were colored black to induce a greater voltage drop. These worked nicely when the web traveled at low speeds; however, when the web traveled at speeds above 50 ft/min, the markers no longer tripped the sensors. To overcome this problem, three markers were placed next

to each other, insuring the photo sensors would respond. These tabs were placed at every $\frac{1}{2}$ inch of pile height as the web was wound on the core (Figure 22).

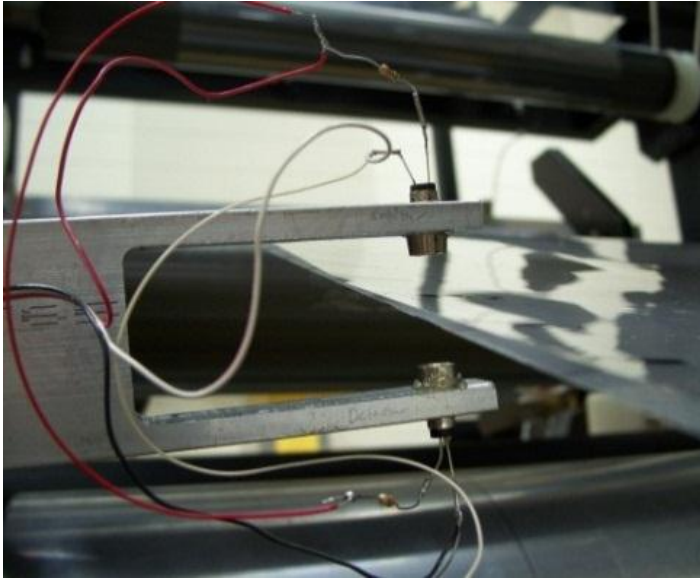


Figure 21 LED emitter and receiver

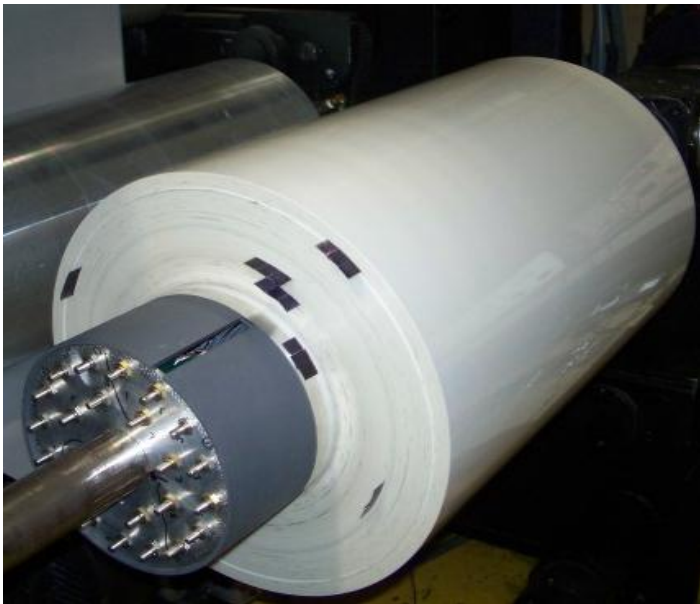


Figure 22 Tabs around roll

4.2 Thickness Measuring Method

The material that was used for all the tests was one of four rolls given the WHRC by Mitsubishi polyester films⁴. The rolls were originally one wide roll which was cut into four different rolls, the roll that was tested was one of the middle rolls, roll 632. Roll 632 is a 24 inch wide white polyester web, that has a nominal thickness of 300 gauge (.003 in).

Once the length of web required to produce enough pressure variation was determined (approximately 3957 ft or 0.8 mile), the thickness variations along that length needed to be mapped out. First, the method of how the MeSys, LED emitter and receiver, and the HSWL worked together will be discussed in further detail. Then the method by which the massive amounts of collected data were reduced and compiled into one excel document will be discussed.

The Mesys was held at a constant CMD position, which corresponded to the midpoint of each of the sectors on the core. Then the web was run at a constant speed while the MeSys took samples at a certain scan rate (millisecond periods). From these two sources of information, the distance in the MD and the thickness at that location in inches could be found using the following equation

Eqn (1):

$$MDpos = \frac{spd}{5}(time - startTime). \quad (1)$$

Again, the markers on the edge of the web were read by the LED system, giving location references, which thereby insured that the same MD locations were recorded for each CMD step of the MeSys.

Once the method was proven, the next step was to determine how many samples were needed to obtain a good representation of the web thickness variation. To answer this question, a 233-inch

⁴ Mitsubishi Polyester Film, inc. 2001 Hood Road, P.O. Box 1400, Greer, SC 29652 ph. 864-879-5000, <http://www.m-petfilm.com/america/>

(about 19.5 ft) section of web was scanned at the MeSys’ maximum scanning rate (the period was set to zero) with the minimum speed of the HSWL, which is 5 ft/min. This test resulted in more than 5600 data points, which gave the best possible representation of web thickness along a small distance in one sector with the given equipment variation (See Figure 19 above). Using this data, the optimal machine speed and sampling times could be determined by taking samples from this “full set” of data.

As mentioned before in Kedl’s work [5], he used an averaged thickness for each wrap in their finite element models of core pressure. Using the same approach, approximate lengths of each wrap were made and the corresponding thicknesses were averaged with the full set of data. As an illustration, the circumference (total length of one wrap) for the first wrap around the core would be $2 \pi r$, where r is the radius of the core (4 inches), or approximately 25 inches. For all the other layers, the radius has grown by the thickness of the web, and the equation would become

$$2 \pi (r + (\text{wrap\#} * \text{thickness})). \quad (2)$$

The nominal thickness was used instead of the actual thicknesses to simplify the initial calculations. The lengths of the 9 wraps are shown in Table 3.

Table 3 Wrap lengths, average thicknesses, and number of points

Average Thickness								
Layer	Wrap Length (in)	Full Data (gauge)	Every 2nd (gauge)	Every 5th (gauge)	Every 10th (gauge)	Every 15th (gauge)	Every 20th (gauge)	Every 25th (gauge)
1	25.142	298.719	298.708	298.744	298.686	298.726	298.919	298.646
2	50.294	300.286	300.301	300.276	300.305	300.243	300.200	300.229
3	75.445	296.951	296.929	296.942	296.909	296.994	296.882	296.966
4	100.597	298.731	298.736	298.737	298.753	298.768	298.764	298.663
5	125.749	299.503	299.503	299.492	299.476	299.522	299.455	299.442
6	150.900	297.576	297.581	297.587	297.587	297.565	297.566	297.509
7	176.052	297.391	297.398	297.386	297.365	297.416	297.339	297.435
8	201.203	300.301	300.299	300.311	300.304	300.267	300.248	300.402
9	226.355	299.956	299.944	299.956	299.936	299.971	299.975	299.920
	# pts	5616	2808	1123	562	375	281	225
	L/#pts	0.041	0.083	0.207	0.415	0.621	0.829	1.036

After the full data was averaged into wrap lengths, it needed to be reduced so that less data could be collected for the full scale testing. To do this, a VBA program was written that took every specified number from the full set of data, always beginning with the first. For example, if every 5th was specified, then the 1st, 6th, 11th... etc. data point would be pulled from the full data. Then, the thicknesses were averaged in the same manner as before and compared with the full set of data (see Table 3). Also shown in Table 3 is how many points were required to map out the full length of sample web. The total length was divided by this value, which gave how much of an inch was between points. For example, if every 25th point was taken, there would be about an inch between points. A distance of one inch between data points was selected because it provided a good balance between representing the data and minimizing the number of samples taken.

Once distance between points was known, a relationship between the sampling speed of the MeSys and the HSWL needed to be determined so that the data could be collected as fast and accurately as possible. If the HSWL were to go at 20ft/min, it would take approximately 4 hours for 3957 ft of web to be wound. By varying the MeSys sampling rate and varying the web speed, a table was created to find the optimum sampling/speed relationship (Table 4). The combination that was chosen was running the HSWL at 80 ft/min and having the MeSys take samples every 50 milliseconds. With this combination, the time required for one test was close to an hour.

Table 4 MeSys HSWL relationship

		Web Vel (ft/min)							
		40	50	75	80	85	90	95	100
in/samp	1	125.00	100.00	66.67	62.50	58.82	55.56	52.63	50.00
	0.95	118.75	95.00	63.33	59.38	55.88	52.78	50.00	47.50
	0.9	112.50	90.00	60.00	56.25	52.94	50.00	47.37	45.00
	0.85	106.25	85.00	56.67	53.13	50.00	47.22	44.74	42.50
	0.8	100.00	80.00	53.33	50.00	47.06	44.44	42.11	40.00
	0.75	93.75	75.00	50.00	46.88	44.12	41.67	39.47	37.50
time(min)		104.76	83.81	55.87	52.38	49.30	46.56	44.11	41.91
Time(hrs)		1.75	1.40	0.93	0.87	0.82	0.78	0.74	0.70

With the distance between samples in the MD known, the distance between data points in the CMD needed to be determined. To do this, CMD scans traversed the whole width of the web. When traveling from sectors 1 to 24, the scan was called a “Zig;” then when traveling back from sector 24 to 1, the scan was called a “Zag.” Using a similar method as above, different CMD distances were taken from the full data and their thicknesses averaged. This is the distance the MeSys would use as it stepped across the web. For clarity, only the Zig data is presented for tabs 3 and 8 in Figures 23 and 24.

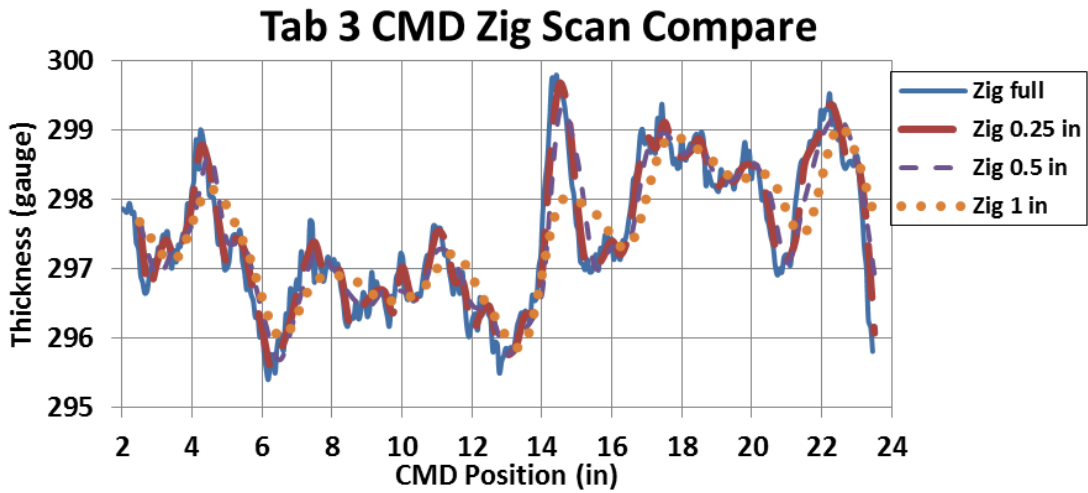


Figure 23 CMD scans comparing sampling distances for Tab 3

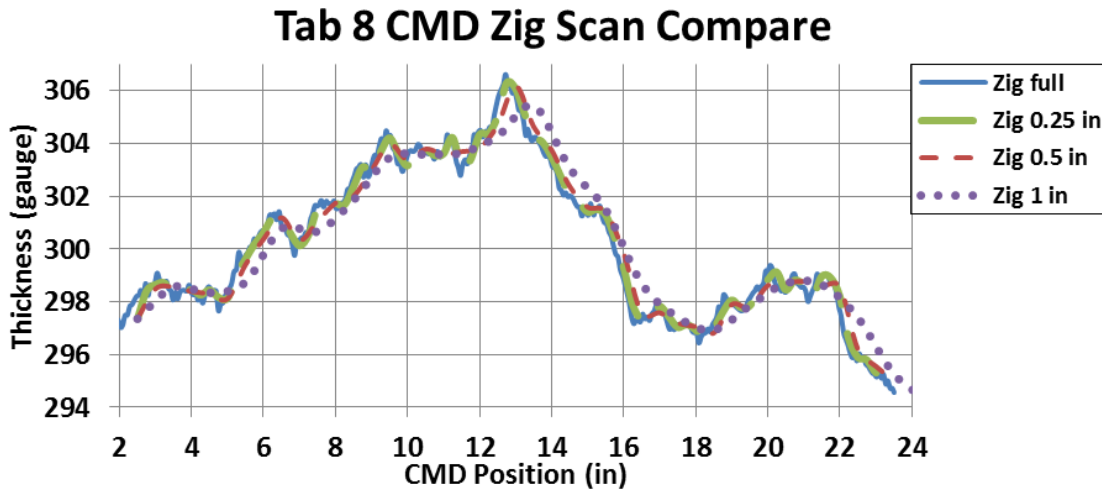


Figure 24 CMD scans comparing sampling distances for Tab 8

Wanting to obtain the best representation of the web without having to perform tests longer than an hour, it was decided to step the MeSys in one-inch increments in the CMD, centered on each sector, because one-inch steps modeled the thicknesses decently. Even with taking data every inch in the MD, there were still approximately 60,000 data points for one sector. This created a problem because not all the data could be stored in one excel file, which was needed for the analytical model. Thus, a similar process as before was used to further reduce the data; however, the actual average thickness for each layer was used as opposed to the nominal thickness. This reduction work was done by Mollamahmutoglu and resulted in 1277 layers of web on the roll.

Once the relationship between the HSWL and the MeSys had been determined, thickness scans were made in the MD. The process went as follows: the MeSys was calibrated and moved to the middle of a sector; sampling was started; and then the HSWL was turned on. By the time the first tab went through the LED sensors, the HSWL was up to speed. After all nine tabs had passed through the LED, the HSWL and MeSys were turned off. Then, the HSWL was reversed, and the MeSys was recalibrated for the next test and parked in the middle of the next sector. The data before the first tab was discarded, and then using the same equation as before ($MDpos = \frac{spd}{5}(time - startTime)$), the distance along the MD was found.

4.3 Thickness Measuring Results

The thickness data was collected by holding the MeSys in the middle of one of the sector locations, and then running the HSWL at 80 ft/ min and sampling with the MeSys at a sampling rate of 50 milliseconds. After the length of web was sampled, the roll was rewound, and the MeSys was recalibrated and stepped to the middle of the next sector. This process yielded 1,440,000 thickness values, which were reduced, and ultimately used in Maxiwinder.

To better understand how the thicknesses of the web acted, the thicknesses for each sector were averaged and plotted together (Figure 25). The first and last sectors were removed because the

readings were unrealistic, which was attributed to the MeSys not behaving well on the edges. The MeSys is known to behave poorly near the edge of a web where ultrasound may pass around the web edge. This error is common to the Beta gauge as well.

The average thickness plot had a similar shape as the previous winding tests, except for sectors 6, 8, and 10.

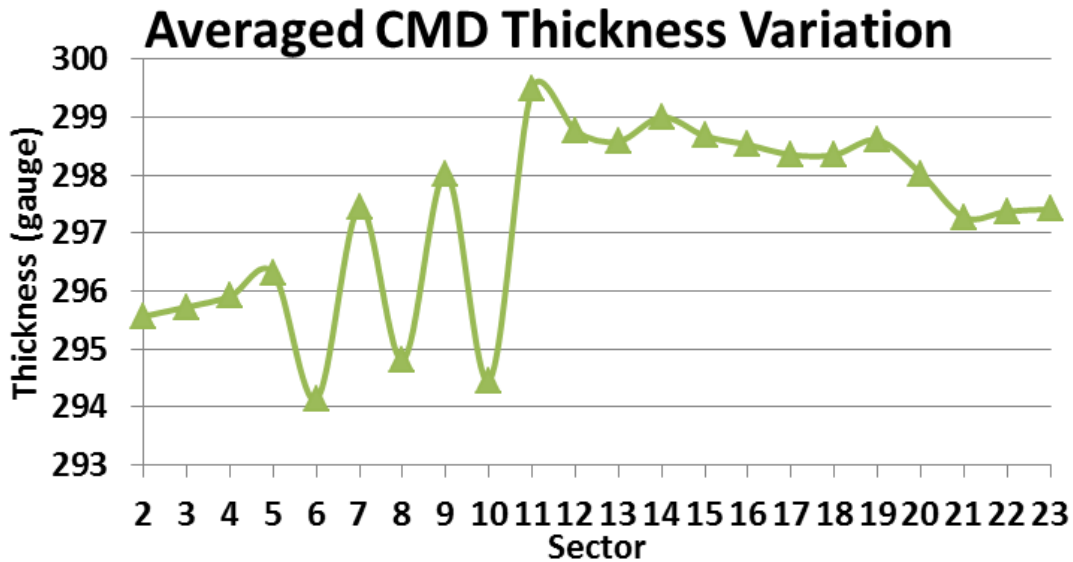


Figure 25 Averaged CMD thickness variation

In an effort to validate the thickness data, the CMD scans from above were compared to the MD scans at the tab locations. From the MD scans, the thicknesses at the tabs were taken and combined into a “composite CMD scan.” Thickness data was extracted from the full CMD scans where the CMD location matched up with where the MD scans were taken. As an example of these tests, sectors 3 and 8 are shown below (Figure 26). From this test, it became apparent that sectors 6, 8, and 10 were anomalies. They were therefore rerun, and the plots were regenerated using the new data for these sectors (Figure 27).

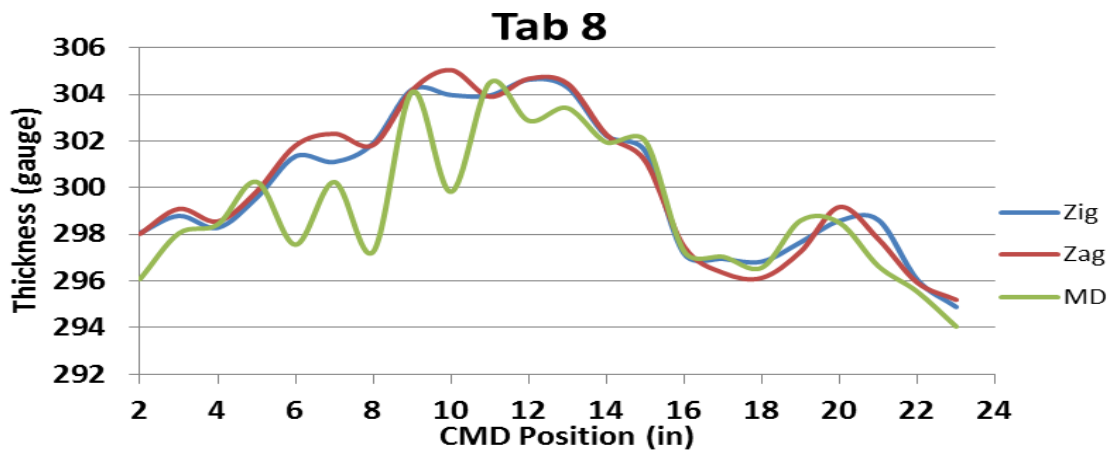
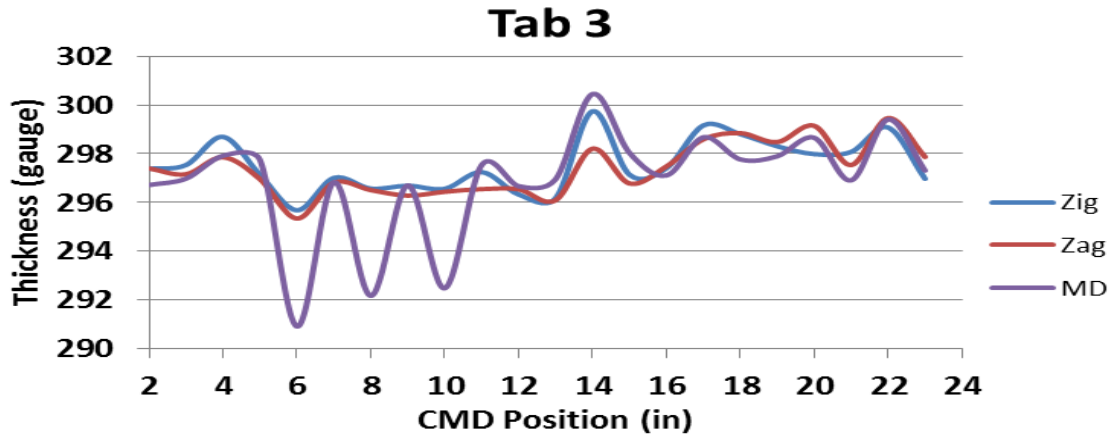
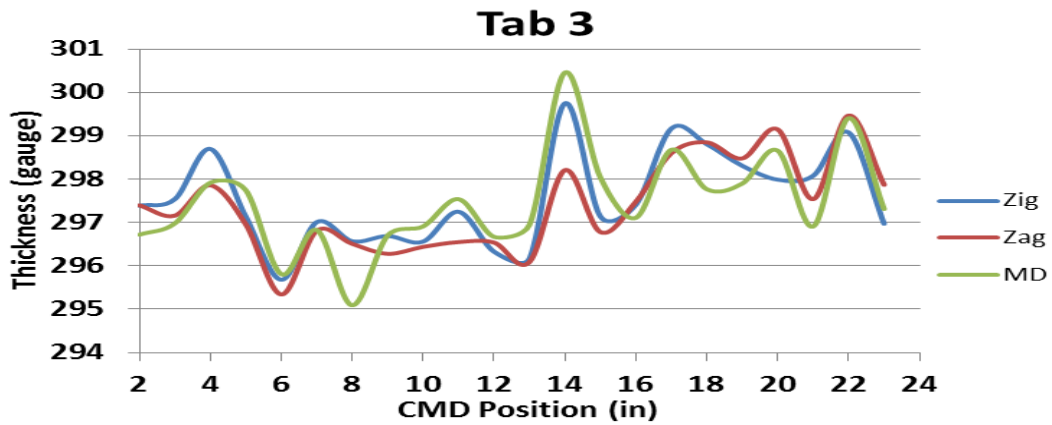


Figure 26 Composite CMD scan from MD scans compared with Zig and Zag of CMD scans



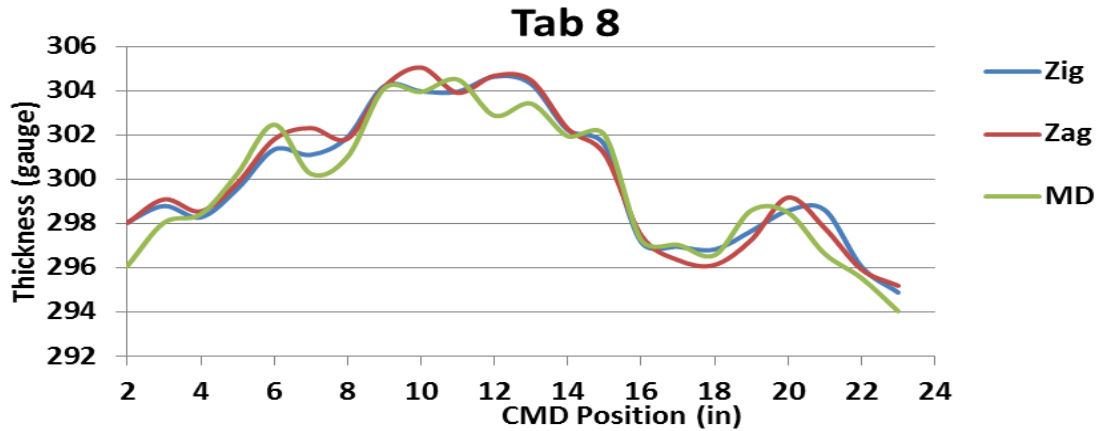


Figure 27 Composite CMD scan with new sectors 6, 8, and 10

Once the thickness data was corrected and compared well with the CMD, all the thicknesses for the sectors were averaged for the 4 inches of pile height and are shown below in Figure 28. Also included in the plot are Mollamahmutoglu’s original thickness scans, which were obtained using a Beta gauge that scanned in a diagonal pattern. These readings were interpolated to get a thickness profile in the MD [8] which resulted in 2,848 thickness values. Since neither measurement system works well near the edges, the edge values were obtained by using a two point linear interpolation with the values around it. Mollamahmutoglu’s original scans are referred to as “Mitsubishi Beta Gauge” on the plot. It was an average of 8.64 gauge points higher, so it was adjusted down for better comparison.

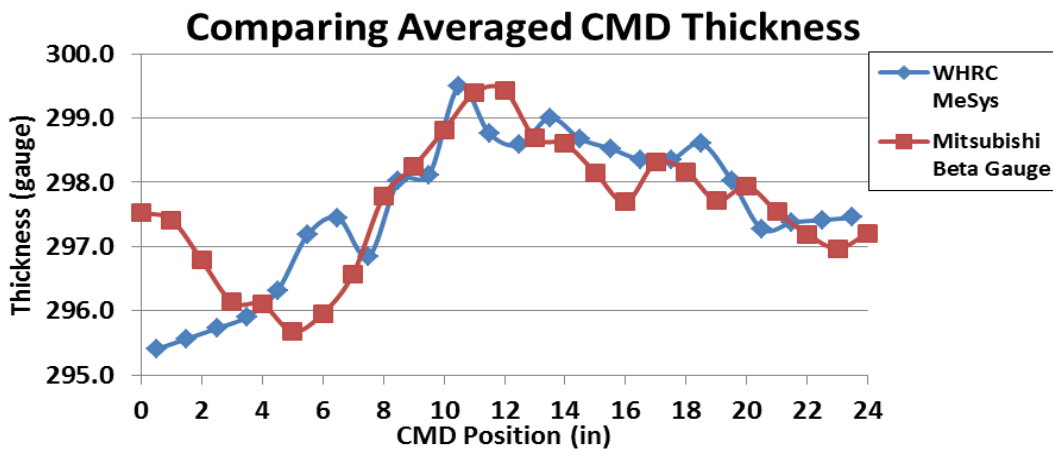


Figure 28 Corrected averaged MeSys thickness data compared with original Beta gauge thicknesses

A contour map of the thicknesses across the whole web, which were used in Maxiwinder is shown below (Figure 29).

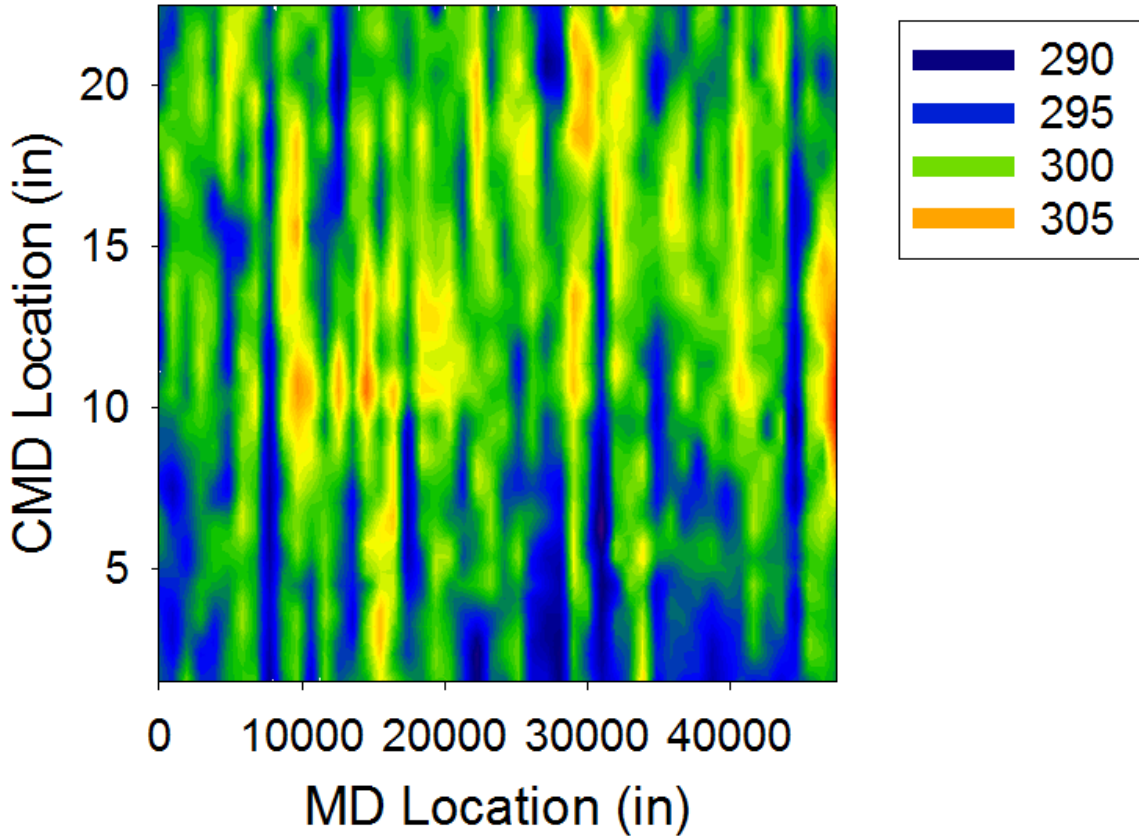


Figure 29 Contour plot of MeSys thicknesses data

As seen from above there is a lot of thickness variation over the length and width of the web

Figure 29. The Beta gauge scan and the MeSys have decent agreement in sectors 8 through 24, but on the other sectors 1-8 there is not much agreement at all Figure 28.

4.4 Material Properties

To most accurately model the polyester web in the simulation, accurate material properties were needed. Two different material property tests were performed on the material. First, a stretch test was completed, from which the material's Young's modulus in both the MD and CMD (E_{wt} and E_{wz} , respectively) could be determined. Then, a compression test was performed to find the web's compressibility in the radial direction, the radial modulus (E_r)

4.4.1 Young's Moduli E_{wt} and E_{wz}

In order to find the material's modulus, a length of 24 feet of web was cut into six-inch sectors, allowing for four separate stretch tests. This insured that the web's modulus did not change in the CMD. Each sector was then rolled out on the ground with one end taped to the ground. The other end had a thin piece of metal taped into a loop with a string attached to it (Figure 30). The string helped ensure that the force would act down the center of each strip of web. A force indicator was hooked onto the string, and a paper was taped on the floor under the web. After pulling the slack out of the web, the indicator was zeroed, and an initial mark was placed on the web and paper. Then the web was stretched in five-pound increments, up to 30 pounds, and a mark was placed on the paper, coinciding with the mark on the web.

This same test was performed for each of the strips. The length that the web was stretched was then measured, giving ΔL , and then divided by the total length of the web, L , which gave the strain ($\epsilon = \frac{\Delta L}{L}$). The stress was found by dividing the force over the cross sectional area. ($P = \sigma = \frac{F}{A_c}$) These two values were plotted against each other in Excel, and the trend line was also plotted (Figure 35). The slope of the line is the material's modulus, and the average value was $E_{wt}=725000$ Psi, which was also used for E_{wz} .

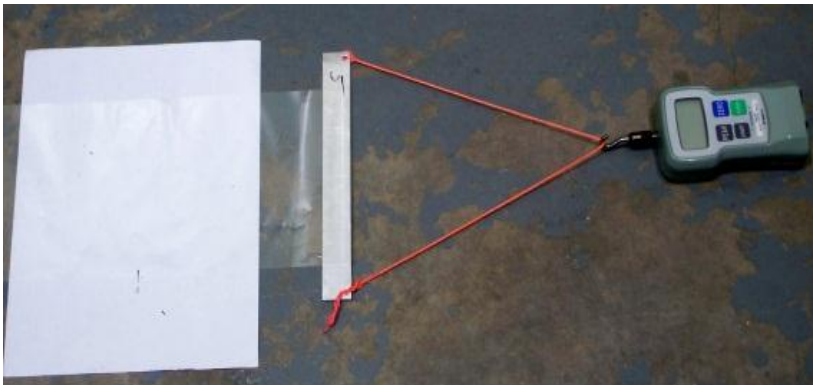


Figure 30 Stretch test setup

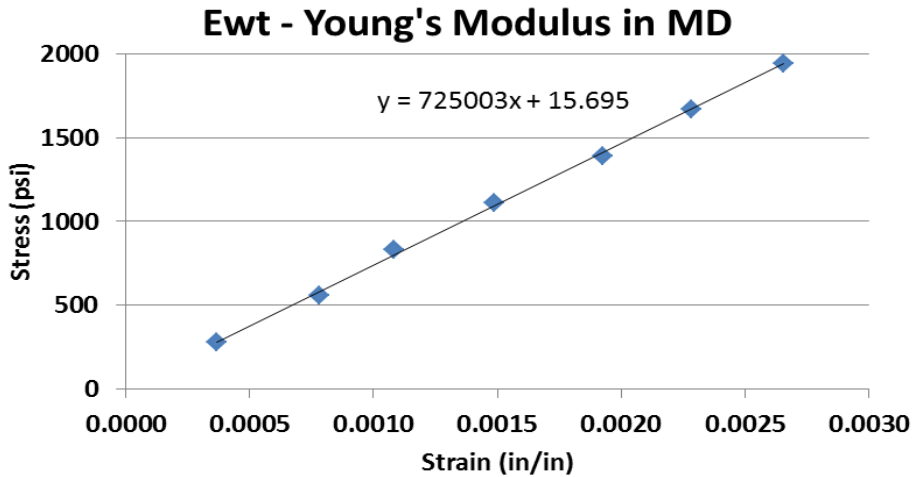


Figure 31 Stretch test plot

4.4.2 Radial Modulus E_r

The second material property test, the compression test, was then performed. The six-inch strips from Young's modulus tests were cut into seven-inch pieces and stacked on top of each other until a one-inch pile height was achieved. These were loaded into a servo-hydraulic testing system made by Instron (Figure 32). This machine is capable of developing 55,000 lb of load in either tension or compression.

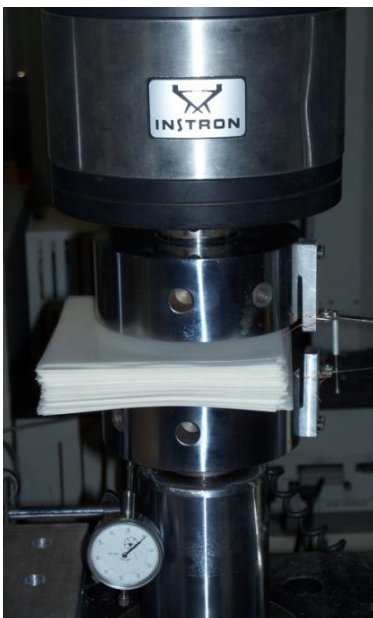


Figure 32 Instron compression test

Again, both the force and displacement were recorded, from which the strains and stresses were calculated in a similar manner as above and plotted (Figure 33). The slope of the line would result in the radial modulus, but since the line is not linear, a curve needed to be fit through the data to get an approximate equation for the data. The stress strain plot was fit with a Pfeiffer curve fit. To find the slope, a derivative of the equation of the line was taken. After solving the derivative, the Pfeiffer coefficients were $k_1=0$ and $k_2=246.5$. The full derivation is included in Appendix.

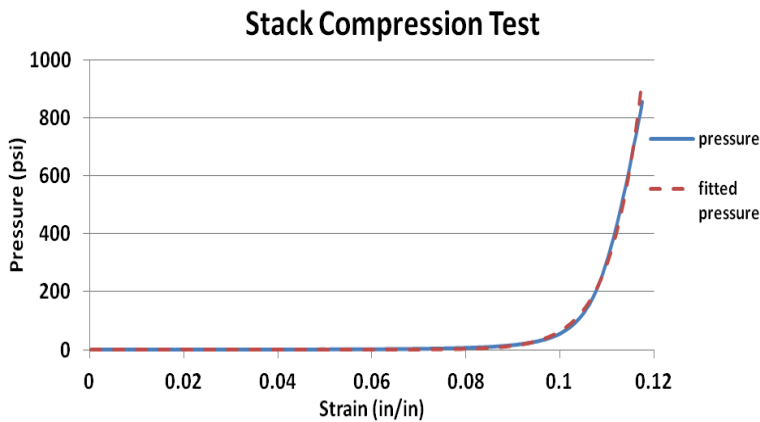


Figure 33 Stack compression test with a Pfeiffer fitted curve

4.4.3 Other Material Properties

Maxiwinder also requires material properties for the core and values for the Poisson's effect (ν) on the web and core. These values were found and used by Mollamahmutoglu in Maxiwinder, and they are reported below, along with a summary of all Maxiwinder's inputs (Table 5).

Table 5 Maxiwinder inputs

Web Properties		Core Properties	
K1	0	E _{core}	10400 ksi
K2	264.5	ν_{core}	0.33
E _{wt}	725 ksi	Core Modulus	600 ksi
E _{wz}	725 ksi	Core router	4 in
ν_{wrz}	0.01	wound roll r	8 in
ν_{wrt}	0.01	r _{nip}	6 in
ν_{wtz}	0.1		

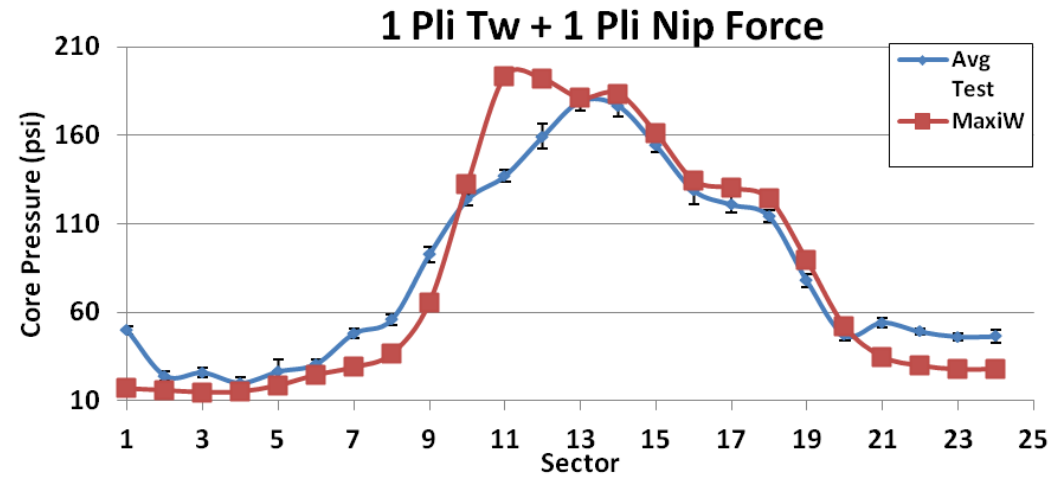
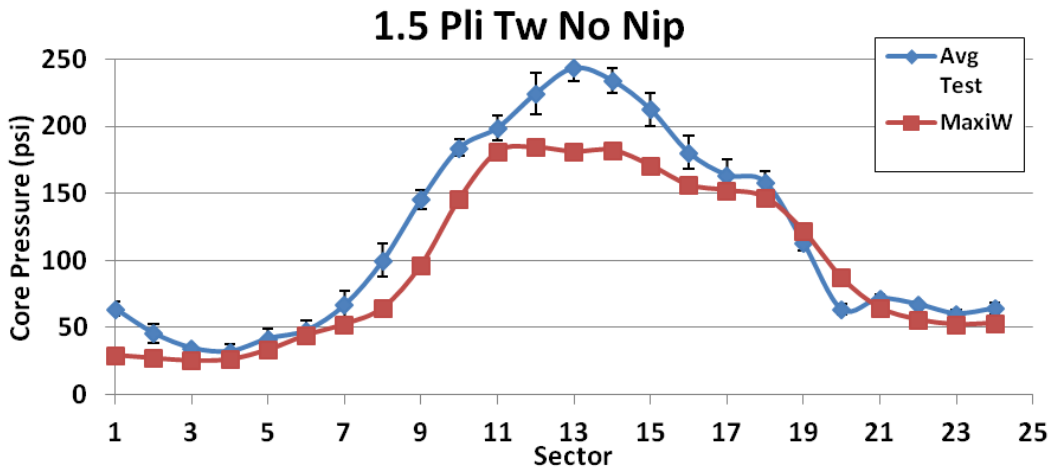
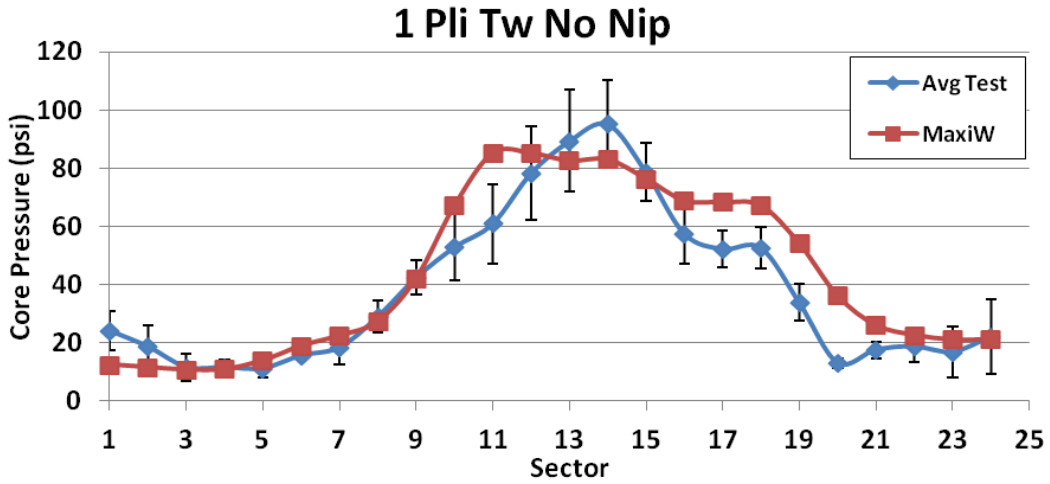
CHAPTER V

COMPARISON OF TEST AND MODEL RESULTS

Once the material properties were defined and the thickness data was obtained, these were used as inputs in Maxiwinder. The following plots show the average winding tests and outer lap radius results plotted with the outputs from Maxiwinder. To obtain the error bars for the average test plots, the standard deviation for a small population was calculated at the same CMD location for each tension and nip load setting using Excel function "=stdevp" in Excel 2007. For example, with the values for sector one of the 1.5 pli Tw + 1 pli nip force pressure case as 101.73, 100.56, and 77.62, the stdevp of these numbers is 11.098. The average of these values was also taken, giving 93.30 psi. These same calculations were performed for each of the different CMD locations. After plotting the average values, the whole range of stdevp were added as error bars to the data sets. For the profile tests, the data was averaged to 1-inch increments across the core. Maxiwinder does not calculate the hardness.

5.1 Core Pressure Comparison

The pressures from Maxiwinder and the lab tests matched very well (Figure 34).



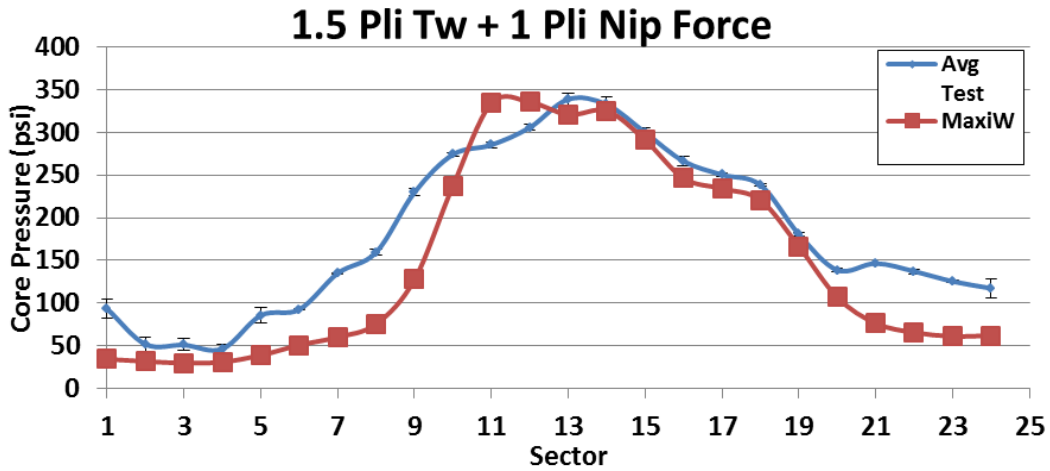
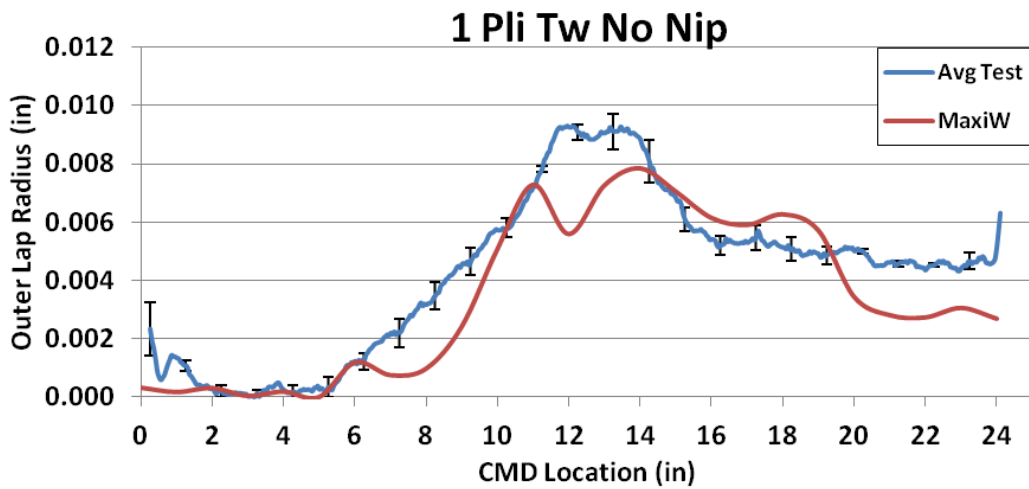


Figure 34 Core pressure results from tests and Maxiwinder

5.2 Outer Lap Radius Comparison

The outer lap radius of each of the four cases will be shown next; notice that the nipped cases did not model the middle sectors very well (Figure 35).



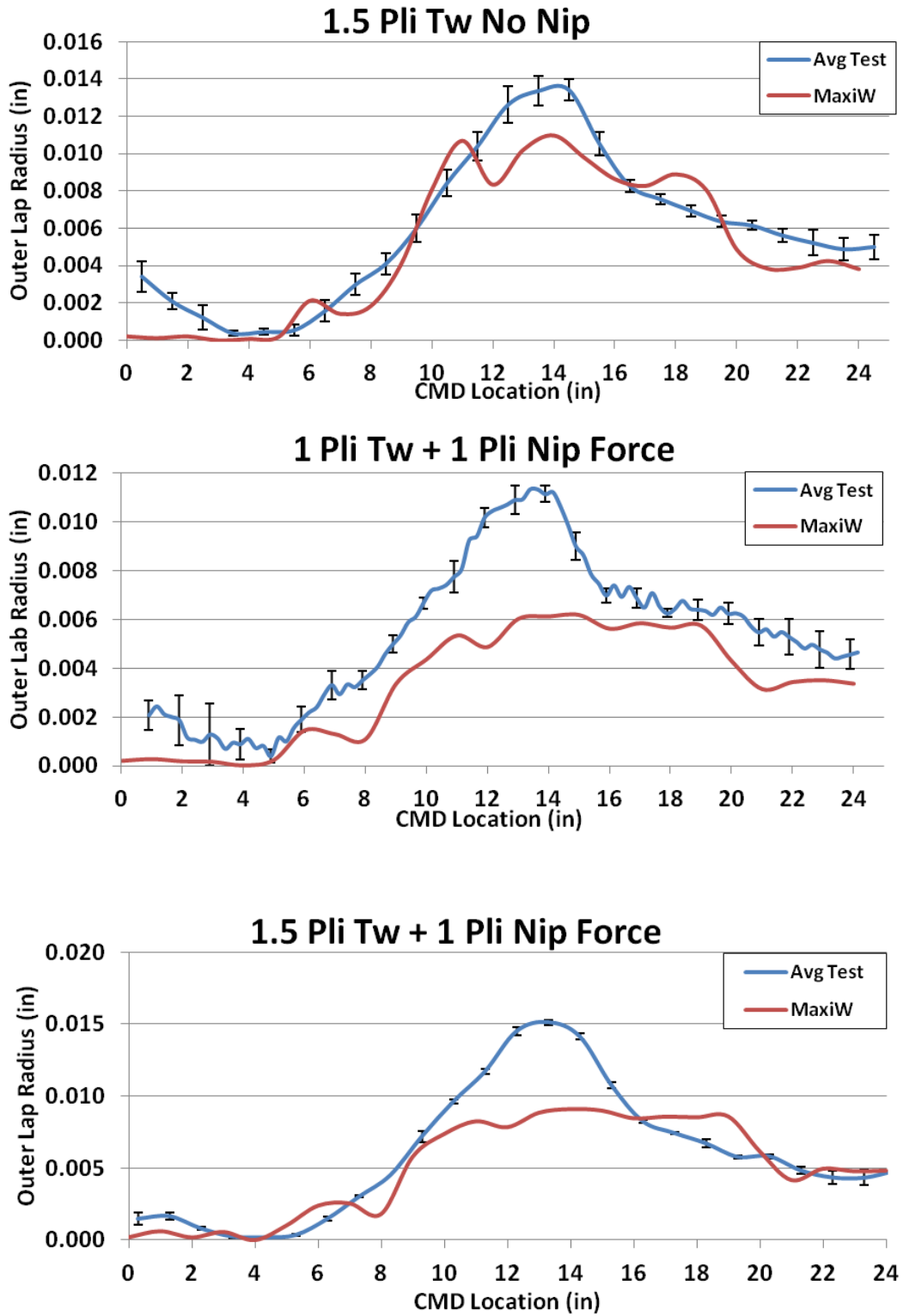


Figure 35 Outer lap radius results from tests and Maxiwider

5.3 MeSys and Beta Gauge Maxiwinder Comparison

A comparison between the MeSys and Beta gauge thicknesses was then made in order to evaluate if and how well they correlated. The tests with 1.5 pli web tension and no nip from both sets of thickness data were chosen for this comparison. Two different variations were made with the thickness data: first, the average thickness of each of the 1277 layers, obtained from the reduction done by Mollamahmutoglu (see page 32), was used; then, the full averaged thickness values for each sector, taken from Figure 28, were used to represent the full MD length. Figure 36 shows the comparison between the two sets of thickness data and the test data for the pressure case. The “Average Test” data set seen on the plot represents the results obtained in the lab, whereas the other data sets are outputs from Maxiwinder.

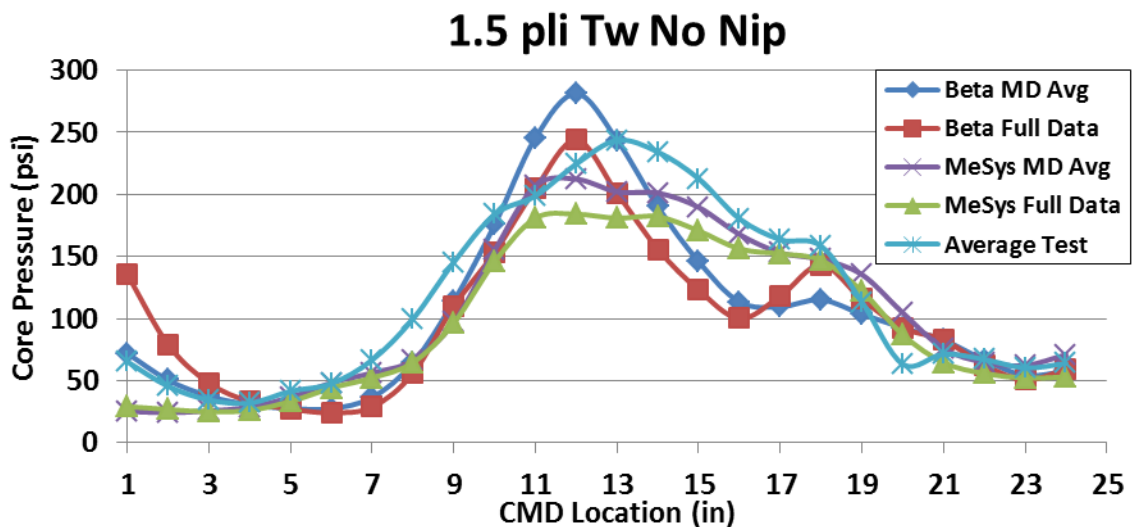


Figure 36 MeSys vs Beta Gauge thickness data for pressure tests using 1.5 pli Tw No Nip

Figure 37 shows both sets of thickness data in comparison to the outer lap radius. The “Beta Full Data” for the outer lap radius case was removed because it had large oscillations and was deemed incorrect.

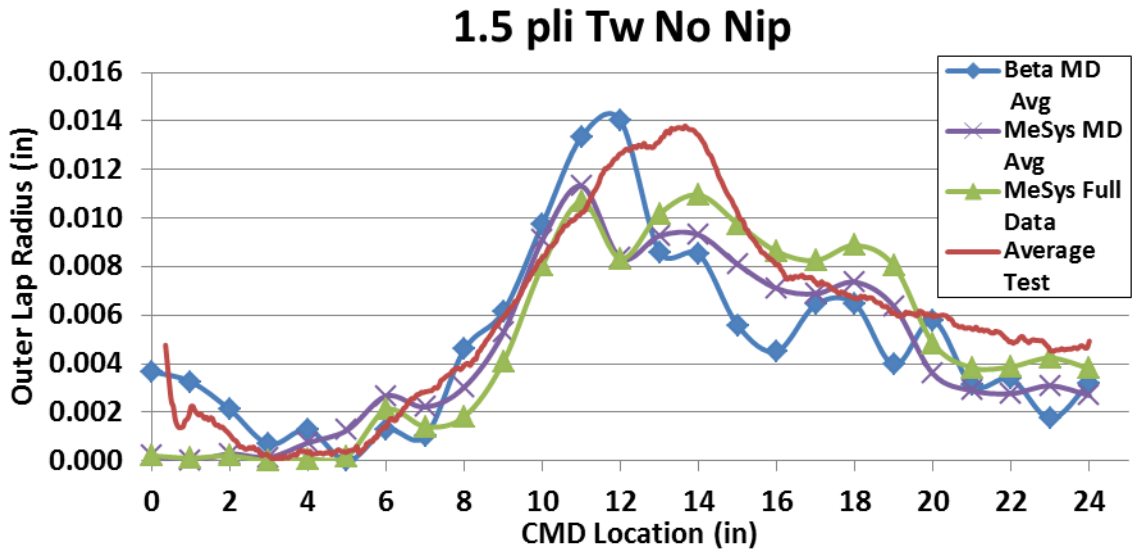


Figure 37 MeSys vs Beta Gauge thickness data for outer lap radius tests using 1.5 pli Tw No Nip

When looking at these results, it was seen that neither set of data modeled the Average Test perfectly. The errors between the Maxiwinder results and the lab tests were calculated by summing the differences between each data set. The results are tabulated in the following tables:

Table 6 shows error in the core pressure and Table 7 shows the error in outer lap radius.

Table 6 Pressure errors

Thickness Method	Averaged Error (psi)
Beta MD Avg	597.81
Beta Full Data	743.07
MeSys MD Avg	431.21
MeSys Full Data	550.66

Table 7 Outer lap radius errors

Thickness Method	Averaged Error (in)
Beta MD Avg	0.0538
MeSys MD Avg	0.0418
MeSys Full Data	0.0324

This shows that, especially for the core pressure tests (Table 6), there is greater error when using the Beta gauge. An interesting comparison is found between the full and average values of both the Beta and Mesys results: it can be seen that the difference is smaller for the MeSys. The errors for the outer lap radius comparison follow the same trend. To better illustrate this, the pressure of each layer was plotted for the whole pile height (Figures 38 and 39). Notice how close the

MeSys MD average and full data lines are to each other; however, the Beta data sets do not follow each other.

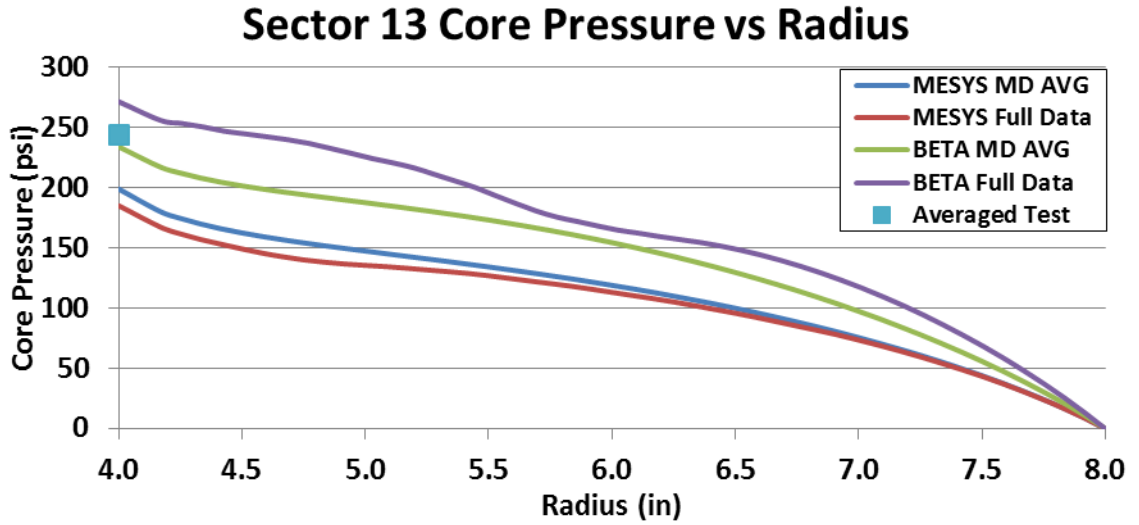


Figure 38 Core pressure throughout the roll radius for sector 13

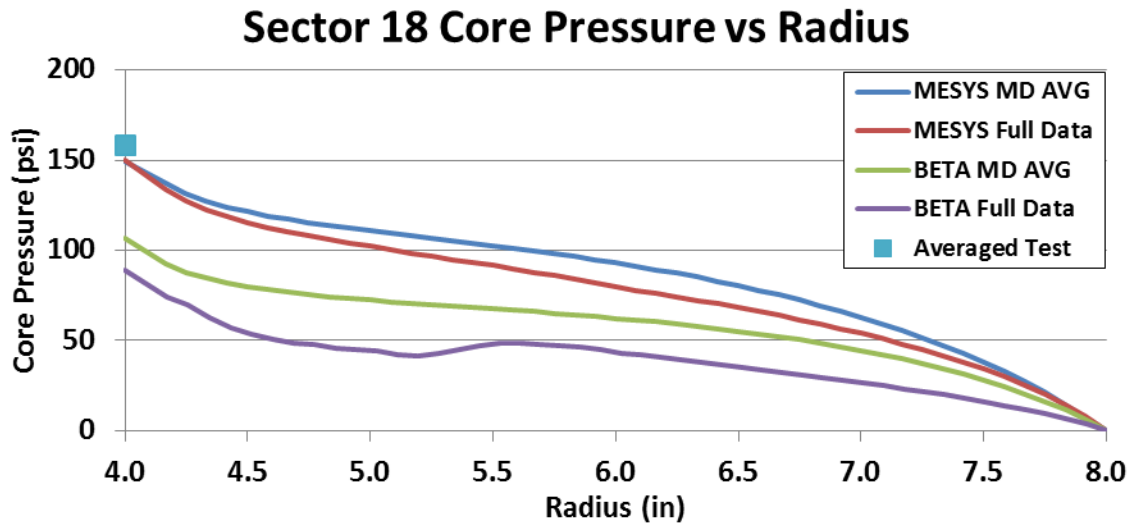


Figure 39 Core pressure throughout the roll radius for sector 18

CHAPTER VI

DISCUSSION OF RESULTS, CONCLUSION AND FUTURE WORK

6.1 Discussion of Results

6.1.1 Winding Tests:

When comparing all of the plots comparing the average pressure, outer lap radius, and hardness, great repeatability was found. The fact that the different types of tests all followed similar patterns gave confidence that the method of collecting data was sound. However, there were some slight inconsistencies within the hardness test. This can be attributed to human error due to the difficulty in insuring that the trigger was pulled at same rate and pressure for each test. It was also difficult maintaining the Rho meter in a tangent position to the roll.

6.1.2 Thickness Tests:

The MeSys is a highly accurate, non-contacting method for collecting thickness data, as was seen by the repeatability of thickness data (Figure 19) and the noise test (Figure 20). Given the matching data from the CMD and the “composite CMD,” which was compiled from the MD scans, the method of stepping across the web in the CMD while taking data in the MD was proven accurate (Figure 27).

It was questioned, “What caused sectors 6, 8, and 10 to be off so much, and what was done to “fix” the problem when they were re run?” The answer to these questions is most likely calibration. Calibrating the MeSys needs to be done with extreme precision. The process includes

manually lining a point on the web with a mark on the roller (which was also lined up with the bearing housing) and then applying 1 pli web tension and running the MeSys calibration function. The MeSys calibration function was performed as described above. The point on the web needed to be exactly the same every time due to the non-uniformities within the web. If calibration of the MeSys was performed at different points there could be an offset between the different sectors. For example, if the MeSys was calibrated to a 310 gauge point on the web, the rest of the scan would be shifted lower. Similarly, if calibration was performed at a point with a gauge of 290, the rest of the data would shift higher. One possible solution for this problem could be to perform calibration off the web on a known sample that would be under constant tension, and under the same environment as the rest of the web.

The MeSys uses an ultrasonic sensor. Therefore, it is also a possibility that conditions in the room could affect the sound waves between the emitter and the receiver by changing the speed of sound.

6.1.3 Maxiwinder and Winding Tests Results:

By using the method of thickness testing mentioned above, the thickness profile in both the MD and CMD of the web were completely mapped out, which had never been done with such accuracy (Figure 29). However, it was necessary to determine whether taking so much data was necessary. After comparing the MeSys Maxiwinder results to the lab tests, good agreement was found in all the cases except for the outer lap radius with nip tests. To continue investigating the accuracy of Maxiwinder, the MeSys results were plotted against the Beta gauge results and compared (Figure 37). It was seen that both MeSys data sets correlated with the test data more closely than the Beta gauge data. In attempt to evaluate the error of each data collection method, the difference in error between the averaged and full data for each method was compared. Because so much data was collected with the MeSys (60,000 data points per sector), the

difference in its error was smaller than with the Beta gauge (119.5 psi versus 145 psi, respectively). The larger Beta gauge error can be explained by the lack of thickness data due to the diagonal scanning pattern, which gave only 2,848 thickness values. The fact that the MeSys collection method still has a considerable error raises the question of whether the slight improvement in the Maxiwinder results with the MeSys thicknesses justifies the cost of collecting so much data. To highlight this, more than 27 hours were spent in data collection, including the time to re run sectors 6, 8, and 10; while on the other hand, the Beta gauge data was collected in about two hours.

6.2 Conclusion

Throughout this paper, the methods for collecting core pressure, outer lap radius, and the hardness were developed. After multiple tests were conducted for each of these tests, good repeatability was found. Each set of data also seemed to follow the same shape. The method of collecting data, therefore, was verified with these results.

It was possible to accurately map out the thickness of a length of web in the MD for each of the 24 sectors on the segmented core. These MD thickness scans were verified by doing CMD scans at the tabbed locations coinciding with a ½-inch of pile height. Composite CMD scans were created from the MD scans at the same locations. In order to get the most accurate thickness data, it is very important to have proper calibration between the MD scans.

The outputs from Maxiwinder were verified by comparing them to the results of the four winding tests' tensions and loads. It was also determined that obtaining thickness data for every square inch of web does improve the outputs of Maxiwinder, but the cost of time for that accuracy must be weighed. For example, if one wants to know the pressures on the core and the outer lap radius, diagonal scans with a thickness gathering instrument would be sufficient. However, if a printing

or coating web process was being done and accurate thickness data was needed, the methods detailed throughout this paper could be employed successfully.

6.3 Future Work

As this work progressed, questions and/or problems arose that should be researched more fully.

6.3.1 Winding Tests:

- Inconsistencies within the hardness testing suggest a need to improve the method of determining the hardness of the roll, eliminating as much human error as possible.
- Research should be performed to explain the existence of differences between test data and Maxiwinder for the nip outer lap radius tests.

6.3.2 Thickness Tests:

- Investigating environmental effects on the speed of sound could help illuminate problems with the MeSys calibration. How do room conditions like temperature, humidity, and pressure affect the speed of sound, and thus the thickness reading? In order to investigate the effect of temperature, the following should be considered: If treating the air as an ideal gas, the speed of sound is calculated by $c = \sqrt{\kappa RT}$, where κ is the ratio of specific heats, which is a constant 1.4; R is the gas constant; and T is absolute temperature. [Ref 11] The room with the HSWL has, at best, a variation in temperature of ± 1.5 degrees Fahrenheit. Using this information and the equation for the speed of sound, if the temperature ranged from 68.5 to 71.5 degrees Fahrenheit, the speed of sound would range from 1129.05 to 1132.24 $\frac{ft}{s}$.
- Developing a fail proof method for consistent calibration of the MeSys would remove variability in calibration.

- Speeding up the collection times while still maintaining accuracy in the data would make it possible to perform more MD scans in less time.

REFERENCES

- [1] Good, J. K., and Roisum, D. R. Winding: Machines, Mechanics, and Measurements, DEStech Publications, INC., 2007
- [2] Hakiel, Z., "Nonlinear model for wound roll stresses," *Tappi Journal*, vol. 70, pp 113-117, May 1987.
- [3] Hakiel, Z., "On the effect of width direction thickness variations in wound rolls," Proceedings of the First International Conference on Web Handling, pp. 79-98, 1991. WHRC, Oklahoma State University.
- [4] Cole, K.A. and Hakiel, Z., "A Nonlinear Wound Roll Stress Model Accounting For Winding Thickness Non-uniformities", AMD vol 149, Web Handling -1992, American Society of Mechanical Engineers, 1992, pp13-24
- [5] Kedl D. M., "Using a two dimensional winding model to predict wound roll stresses that occur due to circumferential steps in core diameter or to cross web caliper variation," Proceedings of the First International Conference on Web Handling, pp. 99-112, 1991.WHRC, Oklahoma State University.
- [6] Mollamahmutglu, C., and Good, J. K., "Axisymmetric Wound Roll Models," Proceedings of the Tenth International Conference on Web Handling, Oklahoma State University, Stillwater, OK, June 2009, pp 105-130
- [7] Mollamahmutglu, C., "A 2D Axis-Symmetric Wound Roll Model Including Nip Effects" Doctor of Philosophy Dissertation. Oklahoma State University, Stillwater, Oklahoma. Dec. 2009

- [8] Precision DC Gaging Transducers Retrieved June 3, 2012 from
<http://www.omega.com/Pressure/pdf/LD500.pdf>
- [9] Rhometer- Theory (2010) Retrieved June 3, 2012 from
<http://millassist.com/index.php/rhometer-theory>
- [10] Thickness Gauge USM-200. Retrieved June 3, 2012, from
http://www.mesys.de/eng/html/usm200_ultrasonic_scanner.html
- [11] Speed of Sound Formulas Retrieved June 3, 2012, from
http://www.engineeringtoolbox.com/speed-sound-d_82.html

APPENDIX

Radial Modulus Derivation

The initial guess of $P = \sigma = k_1 e^{k_2 \varepsilon}$ was used and then the initial conditions of both strain ε and pressure P being zero were substituted into the equation. In order to satisfy the boundary conditions the final equation for pressure was

$$P = k_1 e^{k_2 \varepsilon} - k_1 \quad (\text{A.1})$$

Taking the derivative of A.1 gave

$$E_r = \frac{dP}{d\varepsilon} = k_2 k_1 e^{k_2 \varepsilon} \quad (\text{A.2})$$

Which can be simplified by substituting A.1 into A.2, it becomes

$$E_r = k_2(P + k_1) \quad (\text{A.3})$$

From there equation A.1 was put into an excel document with assumed values for k_1 and k_2 , the error was taken between the experimental pressure and the curve fitted value.

Then the error term was summed. With the excel sheet set up with the measured strains and the curve fitted pressures the values of k_1 and k_2 were minimized using the excel solver function. The values of k_1 and k_2 were found to be zero and 246.4 respectively, these were used in equation A.3 to find the radial modulus E_r .

VITA

Jared William Gale

Candidate for the Degree of

Master of Science

Thesis: WINDING EXPERIMENTS ON NONUNIFORM THICKNESS WEBS

Major Field: Mechanical and Aerospace Engineering

Biographical:

Education:

Completed the requirements for the Master of Science in your Mechanical and Aerospace Engineering at Oklahoma State University, Stillwater, Oklahoma in July, 2012.

Completed the requirements for the Bachelor of Science in your major at Brigham Young University - Idaho, Rexburg, Idaho in 2009.

Name: Jared William Gale

Date of Degree: July, 2012

Institution: Oklahoma State University

Location: Stillwater, Oklahoma

Title of Study: WINDING EXPERIMENTS ON NONUNIFORM THICKNESS WEBS

Pages in Study: 54

Candidate for the Degree of Master of Science

Major Field: Type Field Mechanical and Aerospace Engineering

Scope and Method of Study:

Webs have non-uniformity in thickness that results from the processes by which the webs are made. Webs are stored in the form of wound rolls. The stresses in the wound roll will vary spatially due to the non-uniform thickness. The non-uniformity in thickness may vary over the width and down the length of the web. Winding models have been developed that attempt to capture the spatial variation of the internal stresses as affected by thickness non-uniformity.

This study used experimental methods to validate winding models. Center winding tests were performed with and without nip rollers and core pressure data, outer lap radius, and roll hardness data were collected across the wound roll width. Thickness was mapped over the entirety of the polyester web used in the winding tests and web material properties were measured to provide necessary input for the winding model.

Findings and Conclusions:

Good agreement was found between the test results and the winding model. Better agreement was found in the core pressure than the outer lap radius.

ADVISER'S APPROVAL: J. K. Good
